AAPS PharmSciTech, Vol. 19, No. 8, November 2018 (© 2018)
DOI: 10.1208/s12249-018-1195-9

Research Article

Theme: Lipid-Based Drug Delivery Strategies for Oral Drug Delivery
Guest Editor: Sanyog Jain

Nano-lipid Complex of Rutin: Development, Characterisation and *In Vivo* Investigation of Hepatoprotective, Antioxidant Activity and Bioavailability Study in Rats

G. S. Ravi,[1] R. Narayana Charyulu,[1] Akhilesh Dubey,[1,3] Prabhakara Prabhu,[2] Srinivas Hebbar,[1] and Avril Candida Mathias[1]

Received 29 June 2018; accepted 21 September 2018; published online 2 October 2018

Abstract. The current study was aimed to develop an amphiphilic drug-lipid nano-complex of rutin:egg phosphatidylcholine (EPC) to enhance its poor absorption and bioavailability, and investigated the impact of the complex on hepatoprotective and antioxidant activity. Rutin nano-complexes were prepared by solvent evaporation, salting out and lyophilisation methods and compared for the complex formation. For the selected lyophilisation method, principal solvent DMSO, co-solvent (*t*-butyl alcohol) and rutin:EPC ratios (1:1, 1:2 and 1:3) were selected after optimisation. The properties of the nano-complexes such as complexation, thermal behaviour, surface morphology, molecular crystallinity, particle size, zeta potential, drug content, solubility, *in vitro* stability study, *in vitro* drug release, *in vitro* and *in vivo* antioxidant study, *in vivo* hepatoprotective activity and oral bioavailability/pharmacokinetic studies were investigated. Rutin nano-complexes were developed successfully *via* the lyophilisation method and found to be in nanometric range. Rutin nano-complexes significantly improved the solubility and *in vitro* drug release, and kinetic studies confirmed the diffusion-controlled release of the drug from the formulation. The nano-complex showed better antioxidant activity *in vitro* and exhibited well *in vitro* stability in different pH media. The *in vivo* study showed better hepatoprotective activity of the formulation compared to pure rutin at the same dose levels with improved oral bioavailability. Carbon tetrachloride (CCl_4)-treated animals (group II) failed to restore the normal levels of serum hepatic marker enzymes and liver antioxidant enzyme compared to the nano-complex-treated animals. The results obtained from solubility, hepatoprotective activity and oral bioavailability studies proved the better efficacy of the nano-complex compared to the pure drug.

KEY WORDS: antioxidant; bioavailability; hepatoprotective; lyophilisation; rutin.

INTRODUCTION

Herbal drugs are opening new vistas and have been emerging as potential candidates for the treatment of various diseases. Currently, pharmaceutical industries have been concentrating on the phytomedicines because these are more affordable, closely match up with the patient's ideology, concerns about adverse effects of synthetic medicines and lower phytochemical costs. Mainly, the plant secondary metabolites such as alkaloids, glycosides, flavonoids, terpenoids, *etc.* are bioactive compounds with a variety of biological activities. Flavonoids such as curcumin, rutin, diosmin, quercetin, hesperetin, naringenin, mangiferin, *etc.* are polyphenolic compounds that are ubiquitous in nature and possess strong antioxidant activity (1). They also possess anti-inflammatory (2), anticancer (3), hepatoprotective (4), antibacterial (5), antifungal (6) and antiviral activities (7). However, most of the flavonoids manifest limitation in transporting to the biological system because of their inherent properties like poor solubility, low permeability and diffusibility. Particle size, crystallinity and drug derivatisation are also frailty associated with poor bioavailability of these polyphenolic compounds. Rutin also called as quercetin-3-O-rutinoside (Fig. 1) belongs to the flavonol

Guest Editor: Sanyog Jain

[1] Department of Pharmaceutics, NGSM Institute of Pharmaceutical Sciences, Nitte (Deemed to be University), Deralakatte, Mangaluru, 575018, India.
[2] Department of Pharmaceutics, Shree Devi College of Pharmacy, Kenjar, Mangaluru, 570142, India.
[3] To whom correspondence should be addressed. (e–mail: akhilesh@nitte.edu.in)

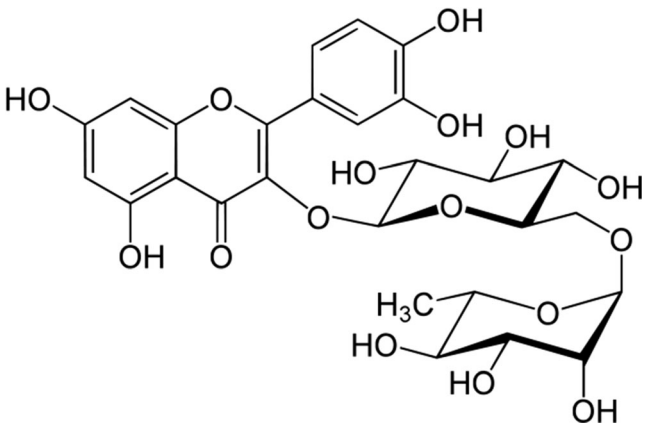

Fig. 1. Chemical structure of rutin

glycosides class, which contains a carbohydrate group (rutinose) which is linked O-glycosidically to one of the flavonoid backbones (2-phenylchromen-4-one, 3-phenylchromen-4-one or 4-phenylcoumarin) and is a polyphenolic compound with excellent therapeutic potential and has a good safety profile. Rutin is one of the ancient drugs that have been used mainly for its antioxidant, anti-inflammatory, cardioprotective, capillary protective, neuroprotective, antithrombotic, anti-ageing and hepatic protective effects.

Despite that rutin has huge therapeutic effects, its phenolic nature makes it polar with poor aqueous solubility and also exhibits low solubility in most of the organic solvents. Poor solubility of the drug affects the dissolution, absorption and thereby bioavailability of the drug on oral administration. Poor absorption and bioavailability of rutin is the main reason for its reduced bioactivity. Hence, the oral dosage regimens normally require a large rutin dose of 500 mg twice a day. These aspects limit the widespread use of rutin by and large. There are two main factors responsible for the poor absorption of rutin: firstly, rutin is having multiple ring structures which is very large to be absorbed by simple diffusion process, and secondly, rutin has poor miscibility with lipids, which hinders it to pass across the lipid-rich membranes of the intestinal simple columnar epithelial absorptive cells called enterocytes. The effectiveness of any herbal formulation depends upon delivering an effective level of active compounds to the desired site. The drug-lipid nano-complexes meet this challenge by markedly enhancing the solubility, absorption and bioavailability of the phytomedicine for better therapeutic activity (8–11). Drug-lipid nano-complexes may be absorbed from the GIT through enterocyte-based transport and to the systemic circulation *via* the intestinal lymphatic system which has a widespread network throughout the body. The advantage associated with lymphatic transport is to bypass the first-pass metabolism and applicable for targeted drug delivery (12,13). Further, as an indispensable constituent of cell membrane, phospholipids play a key role in keeping cell membrane fluidity, which makes it possible that the complex crosses cell membranes without disturbing the cellular lipid bilayers. Identically, the phospholipid complexes are liable to be transported from a hydrophilic environment to a lipophilic environment of the enterocyte cell membrane, then into the cell and lastly into the systemic blood circulation (14).

In the last decade, lipids have gained much interest as carriers for the delivery of drugs with poor water solubility (15). Natural soybean phosphatidylcholine (SPC) and egg phosphatidylcholine (EPC) are considered as effective and safe carriers for clinical applications with biodegradability, good biocompatibility, low toxicity and effective metabolic activity in comparison with their synthetic alternatives (16,17). All these factors suggest that natural phospholipid-based drug delivery systems are favourable systems to achieve better therapeutic activity of rutin.

The main interaction between phospholipid and phytomedicine occurs due to hydrogen bond formation between the polar head of the EPC and the polar functional group of phytomedicine. It is also reported that improved physical stability of the nano-complexes is mainly due to the formation of such hydrogen bonds. Maiti *et al.* developed drug-lipid complexes of curcumin and naringenin in two different studies and reported that nano-complexes have improved the oral bioavailability of curcumin and naringenin (18,19). Likewise, several scientific literatures suggested that the drug-lipid complex improves physical stability, absorption and bioavailability, respectively (20,21).

Therefore, the objective of the present work was to develop rutin:egg phosphatidylcholine nano-complex, a self nano-vesicular pre-concentrate which will convert into a liquid vesicular form on contact with GIT aqueous media. It is anticipated that the rutin nano-complex will gain micellar shape with better stability of the formulation (20). The developed rutin:egg phosphatidylcholine nano-complex was evaluated for its formation through numerous parameters like differential scanning calorimetry (DSC), Fourier transform infrared spectroscopy (FTIR), proton NMR, X-ray powder diffractometry (XRD) and other physico-chemical parameters like particle size analysis, zeta potential, surface morphology, drug content, *in vitro* stability and drug release study. Further, the nano-complex was investigated for its *in vitro* antioxidant activity, *in vivo* hepatoprotective activity and oral bioavailability/pharmacokinetics.

MATERIAL AND METHODS

Materials

The EPC phospholipid 'Lipoid® E 80 S' was a kind gift sample from Lipoid GmbH, Frigenstrasse 4, Ludwigshafen, Germany. Rutin was procured from Sigma-Aldrich, Mumbai. Dimethyl sulphoxide (DMSO), *t*-butyl alcohol, dioxane, methanol and chloroform were purchased from HiMedia Laboratory Pvt. Ltd., Mumbai, India. Acetonitrile, n-hexane, n-octanol, orthophosphoric acid and all other chemicals/reagents were of analytical or HPLC grade.

Animals

The adult male Wistar rats weighing 180–200 g used for the study were obtained from Nitte University Centre for Animal Research and Experimentation (NUCARE), approved by the Institutional Animal Ethics Committee (IAEC) of N.G.S.M Institute of Pharmaceutical Sciences (Approval No.: NGSMIPS/IAEC/MAY-2017/43). Experiments were performed in accordance with the CPCSEA guidelines and approved by the institutional ethics committee. Animals were housed in groups of seven to eight in colony cages at an ambient temperature of 20–25°C and 45–55% relative humidity with 12 h light/dark cycles. They had free

access to pellet chow (Rat and Mice Feed, Krishna Valley Agrotech LLP, Sangli, India) and water *ad libitum.*

Preparation of Rutin Nano-complexes

As a preliminary study, three different methods of preparation of nano-complexes, namely solvent evaporation, salting out and lyophilisation method, were compared. Nano-complexes were prepared by taking the rutin and EPC in 1:2 M ratio. The EPC used was Lipoid® E 80 S. In the first method, the rutin nano-complexes were prepared by solvent evaporation technique, as described by Maiti *et al*. The molar ratios of rutin (0.1% *w*/*v*) and EPC (Lipoid® E 80 S) (1:2) were accurately weighed and refluxed for 5 h at 45 ± 5°C by placing into 250 mL round bottom flask containing 20 mL of dioxane-methanol mixture (7:3). The solvent was then evaporated under vacuum (22). Salting out method was used as the second method of nano-complex preparation. In this method, rutin (0.1% *w*/*v*) and EPC (1:2) were dissolved in 35 mL of the solvent mixture containing DMSO, chloroform and dehydrated ethanol (2:3:2 ratio). The solution was then gently stirred overnight by using a magnetic stirrer, followed by the addition of 75 mL of n-hexane until the formation of precipitate (23).

The lyophilisation was the third method used to prepare the nano-complex. In this method, rutin was dissolved in DMSO (2.5% *w*/*v*) and EPC dissolved in *t*-butyl alcohol (1.5% *w*/*v*). The rutin solution was added to the EPC solution followed by 3 h of stirring on a magnetic stirrer and then isolated by using the lyophilisation process. The above solution was filled in vials and these vials were frozen at − 80°C by keeping in an ultra-low temperature freezer (DW-86L338, Haier-Bio Medical, China) for 4 h. These frozen vials were then placed in the lyophiliser (EBT – 10N, Esquire Biotech, Chennai, India) with a condenser temperature of − 70°C. Lyophilisation was carried out at 40 mbar pressure and a shelf temperature of − 40°C for 24 h. Then, it was subjected to secondary drying at 25°C for another 24 h (24). The samples were taken out from the lyophiliser, and thus, the formed rutin nano-complex was placed in a desiccator over fused calcium chloride at 4°C until further use (25).

Based on the results obtained after the preliminary preparation of the nano-complexes by three different methods, the best developing technique was selected and the influence of formulation variables such as selection of proper co-solvent (chloroform, acetone, methanol, ethanol or *t*-butyl alcohol) and optimum rutin:EPC ratio (1:1, 1:2 and 1:3) was assessed.

Evaluation of Rutin Nano-complexes

Thermal Response

The thermal response of rutin:EPC nano-complex was evaluated by using differential scanning calorimetry (TA Instruments, TGA/DSC - SDT Q600, New Castle, England). The samples were taken in an aluminium crimp cell and sealed, and then it was heated at a speed of 10°C/min from 30 to 300°C in a nitrogen atmosphere (60 mL/min). Thermograms of rutin, EPC (Lipoid® E 80 S), physical mixture of rutin:EPC (1:2) and rutin:EPC (1:2) nano-complex were obtained (26). Thermal response of the formulations F1, F2, F3 and F4 were also obtained.

Fourier Transform Infrared Spectroscopy

An FTIR spectra matching approach was used to determine the possible chemical interactions between the rutin and EPC using FTIR spectrometer (Alpha Bruker, Japan). The ATR method was employed in which a small quantity of the sample was placed below the FTIR spectrophotometer probe. Then the probe was tightly fixed and scanned in the wave number region 4000–500 cm^{-1} to obtain the spectra of samples (27). Samples assessed incorporated rutin, EPC (Lipoid® E 80 S), physical mixture of rutin:EPC (1:2) and rutin nano-complex 1:2 formed by the lyophilisation method, and formulations F1, F2, F3 and F4 were also assessed and interpreted.

Proton NMR (^{1}H-NMR)

^{1}H-NMR spectra of pure rutin, EPC (Lipoid® E 80 S) and selected rutin nano-complex formulation were taken to compare the carbon-hydrogen framework of individual components. Samples were dissolved in DMSO and then transferred to NMR tubes and analysed using 400 MHz FT-NMR spectrometer (Bruker Advance II, Bruker, Rheinstatten, Germany).

X-ray Powder Diffractometry

To study molecular crystallinity, X-ray diffraction patterns of pure rutin, EPC (Lipoid® E 80 S) and selected rutin nano-complex formulation were obtained using X-ray diffractometer (Rigaku MiniFlex 600, Japan). The operation specifications were as follows: 40 kV tube voltages, 40 Ma tube current, K_α lines of copper as radiation source and scanning angle ranging 5–50° of 2θ in step scan mode with 1°/min step width.

Particle Size Analysis and Zeta Potential

The mean particle size (in nm), polydispersity index (PDI) and zeta potential of formulations F1, F2, F3 and F4 were determined by dynamic light scattering (DLS) method using Malvern Zeta Sizer (Malvern Instruments, Malvern, UK). The samples were diluted with distilled water in 1:10 ratio before the measurement. Measurements were performed in triplicates (28).

Surface Morphology

Scanning electron microscopy (SEM) and transmission electron microscopy (TEM) were used to determine surface morphology of the formulated nano-complexes. SEM study was carried out by using a scanning electron microscope (JEOL-JSM 6380LA, Tokyo, Japan). The samples for SEM were prepared by lightly sprinkling the nano-complexes on a double adhesive tape, which was stuck on an aluminium stub. The photographs of pure rutin and selected rutin nano-complex formulation were taken with the help of a SEM analyser (29). TEM was also used to determine the morphological characteristics of selected nano-complex formulation by using a transmission electron microscope (JEM-100S microscope; JOEL Ltd., Tokyo, Japan). The sample was diluted in a 1:20 ratio with distilled water and sonicated for

3 min using a probe sonicator (Vibra-Cell™ Ultrasonic Liquid Processor-VCX130, Sonics & Materials Inc., Newtown, CT, USA). One drop of the diluted solution of rutin nano-complex was then placed on a carbon-coated copper grid, forming a fine liquid film. The film on the grid was negatively stained by the addition of one drop of ammonium molybdate (2% *w*/*w*) in 2% *w*/*v* ammonium acetate buffer (pH 6.8). Excess stain was removed with a filter paper. The stained film was dried in air and observed under a transverse electron microscope and photographs were taken.

Drug Content Analysis

The rutin content in nano-complex formulation was determined by the HPLC method as developed and validated by Sanghavi *et al.* (30) with minor modifications. Weighed quantity (2.5 mg) of the rutin nano-complex formulation (F1–F4) was dispersed in 5 mL of chloroform. Chloroform was chosen due to the reason that the free rutin is insoluble. The solution was filtered through 0.2 μm membrane filters. The free rutin residue which was precipitated out was dried, dissolved in methanol and analysed by HPLC (Prominence UFLC, Shimadzu, Japan) using column C-18, after suitable dilutions. The mobile phase (acetonitrile:orthophosphoric acid, 45:55) was run at a flow rate of 1 mL/min, and the column effluent was detected using an ultraviolet detector (UV PDA detector; SPD-M20A) at 360 nm. For the calibration curve, reference stock solution of pure rutin was prepared at concentration of 1000 μg/mL by dissolving 25 mg of pure rutin in 25 mL of methanol in 25 mL volumetric flask and diluted suitably to get the concentration range of 5–30 μg/mL. The regression equation was found to be $Y = 39{,}267X - 8602$ under a linearity range of 5–30 μg/mL. Retention time was 4.5 ± 0.03 min and the correlation coefficient (r^2) was 0.999.

In Vitro Stability Study

The *in vitro* stability study was performed for the nano-complex at pH 1.2 simulated gastric fluid (SGF) and pH 7.4 simulated intestinal fluid (SIF) containing no enzymes. One milliliter of the formulation was made up to 10 mL with SGF and SIF and incubated for 2 and 6 h, respectively (31). Samples were stirred at 50 rpm at 37°C temperature in a water bath shaker. The samples were then subjected to particle size analysis, zeta potential and polydispersity index study. All the experiments were carried out in triplicate.

Solubility Study

Saturation solubility of pure rutin and selected rutin nano-complex formulation in water and n-octanol was determined by adding an excess amount of sample to 10 mL of solvent in glass vial and capped, stirred at 100 rpm to achieve uniform mixing at room temperature (25–30°C) for 24 h. The resultant solution was centrifuged (R-8C, Remi Elektrotechnik Ltd. Vasai, India) at 5000 rpm for 30 min. The supernatant was filtered through 0.2 μm membrane filter, and after suitable dilution, the samples were analysed by HPLC method. The partition coefficient of pure rutin and rutin nano-complex formulation (F2) in n-octanol/phosphate buffer pH 7.4 was also determined by a conventional method using separating funnel and was calculated using following equation,

$$\frac{C_1}{C_2} = K$$

Where C_1 is the concentration of the drug in the oil phase, C_2 is the concentration of the drug in an aqueous phase and K is an equilibrium constant.

In Vitro Drug Release Study

In vitro drug release from the nano-complex was determined using the dialysis method. The dialysis sacks were washed as per the instruction given by the manufacturer. After proper pre-treatment, one end of the sack was tied and known amounts (10 mg) of pure rutin and rutin nano-complex formulations (F1–F3) (~ 10 mg of rutin) were placed inside the sacks. The other end of the sack was tied and suspended vertically into a beaker placed on a magnetic stirrer with hot plate containing 500 mL of buffer solution of pH 1.2 and pH 7.4 as two different dissolution media in order to mimic the pH of the stomach and a distal part of the small intestine. The pH of the dissolution medium was kept 1.2 for the first 2 h and then replaced with pH 7.4. The content of the beaker was stirred at 100 rpm at 37°C. The samples were withdrawn (5 mL) from the dissolution medium at various time intervals, and the apparatus was immediately replenished with the same quantity of fresh buffer medium to maintain the sink conditions (25). Samples were filtered through 0.2 μm membrane filter and analysed by the HPLC method after the required dilution. The data obtained from the *in vitro* release study was fitted to kinetics release models to understand the mechanism of drug release from the rutin nano-complex.

In Vitro Antioxidant Activity

The free radical scavenging activity of pure rutin and rutin nano-complex formulation (F2) was measured and compared with the activity of standard (ascorbic acid) using stable free radical DPPH (2,2-diphnyl 1-picryl hydrazyl) as per the method described by Jamuna *et al.* with modifications (32); 0.1 mM solution of DPPH in methanol was prepared, and from this, 1.55 mL was added to 3.5 mL methanolic solution of pure rutin and rutin nano-complex of different concentrations ranging from 10 to 50 μg/mL (30). The absorbance of the standard and samples were measured at 517 nm using an ELISA plate reader (AM-2100, Alere Inc., USA). The % DPPH scavenged was calculated using the following formula:

$$\%\text{Inhibition of DPPH} = \frac{\text{Absorption (control)} - \text{Absorption (sample)}}{\text{Absorption (control)}} \times 100$$

In Vivo Hepatoprotective (Liver Function Test) and Antioxidant Activity Studies

Dosing

The adult male Wistar rats were divided into six groups of six animals in each. Group I animals were treated with

distilled water with 1% *v/v* Tween 20 p.o. for 7 days and considered as the normal group. Group II animals were treated with an equal mixture of carbon tetrachloride (CCl_4) and 50% *v/v*, 5 mL/kg olive oil as single dose i.p. on the 7th day. Group III and IV animals were treated with rutin suspension in distilled water with 1% *v/v* Tween 20 at a dose level of 100 and 200 mg/kg, respectively, per day p.o. for 7 days. On the 7th day, a single dose of equal mixture of CCl_4 and olive oil was administered (50% *v/v*, 5 mL/kg, i.p.). Group V and VI animals were treated with rutin nano-complex (F2) equivalent to 100 and 200 mg/kg of rutin, respectively, p.o. for 7 days. A single dose of equal mixture of CCl_4 and olive oil was administered (50% *v/v*, 5 mL/kg i.p.) on the 7th day (23,33,34).

Serum Analysis

Animals have fasted, and after 24 h of intoxication, they were anaesthetised with ether and blood was collected from retro-orbital plexus on the 8th day. Serum was separated by centrifugation (CM-8 PLUS, Remi Elektrotechnik Ltd. Vasai, India). Liver function test (LFT) was performed by measuring serum glutamate oxaloacetate transaminase (SGOT) also known as aspartate transaminase (AST), serum glutamate pyruvate transaminase (SGPT) also known as alanine transaminase (ALT), serum alkaline phosphatase (SALP) and total bilirubin. On the 8th day, after blood collection, animals were sacrificed by cervical decapitation under light ether anaesthesia. The liver was dissected from the animals immediately for biochemical estimation and histopathological observation. The liver was washed in ice-cold saline, and the homogenate prepared in 0.1 M Tris HCl buffer (pH 7.4). The homogenate was subjected to centrifugation and the supernatant was used for the assay of marker enzymes namely reduced glutathione (GSH), glutathione peroxidase (GPx), glutathione S transferase (GST), glutathione reductase (GRD), superoxide dismutase (SOD), catalase (CAT) and thiobarbituric acid reactive substances (TBARS). Protein concentration was determined using purified bovine serum albumin as standard (20,23,34).

Histopathological Studies

Immediately after sacrifice, the liver of the animals was dissected and preserved in neutral buffered formalin. Livers were sectioned and stained with haematoxylin and eosin and examined under a microscope (Zeiss Primo Star Digital, Germany) (22,35).

Oral Bioavailability Studies

The Concentration of Rutin in Rat Serum

For the oral bioavailability study of pure rutin and rutin nano-complex (F2), male Wistar rats weighing 150–200 g were divided into two groups ($n = 6$). All the animals were fasted overnight with access to water *ad libitum*. Group I received a single dose of pure rutin (100 mg/kg, p.o.) and group II received a single dose of rutin nano-complex (~ 100 mg/kg rutin, p.o.). Under ether anaesthesia at predetermined time intervals, blood samples were collected from the retro-orbital plexus in centrifuge tubes and centrifuged at 3000 rpm for 10 min, and serum was separated and kept at − 20°C until further use.

The amount of rutin in the rat serum was estimated by using the HPLC method as developed and validated by Maiti *et al.* (33) with some modifications. Acetonitrile and 0.1% orthophosphoric acid in the ratio 45:55 were used as mobile phase. Flow rate was kept at 1 mL/min. UV PDA detector (SPD-M20A) at 360 nm was used for detection.

Extraction of Rutin from Plasma and Sample Preparation

After attaining room temperature, 1 mL of serum was taken in 10 mL volumetric flask and 5 mL methanol was added. It was shaken vigorously and heated at 75°C for 30 min and volume was made up to 10 mL with methanol. This solution was centrifuged (R-8C, Remi Elektrotechnik Ltd. Vasai, India) at 5000 rpm for 30 min. The supernatant was separated and filtered and 20 μL was subjected to HPLC analysis.

Pharmacokinetic Parameters

The pharmacokinetic parameters such as maximum plasma concentration (C_{max}) and the time required to reach maximum concentration (T_{max}) of rutin nano-complexes were determined based on the plasma concentration-time curve. Other parameters such as area under plasma concentration-time curve from zero to time of the final measured sample (AUC_{0-t}) and area under plasma concentration-time curve from zero to infinity ($AUC_{0-\infty}$), elimination half-life ($t_{1/2el}$), elimination rate constant (K_{el}), clearance (Cl) and volume of distribution (V_d) were calculated using computer software (WinNonlin®, Version 4.1, USA) and compared to the parameters obtained for free rutin. Relative bioavailability (F) is the ratio of total amount of drug absorbed from rutin nano-complex to the total amount of drug absorbed from pure rutin. The amount of drug absorbed (A_{max}) from a dosage form is a function of V_d, K_{el} and $AUC_{0-\infty}$. Therefore, the relative bioavailability (F) was calculated by using the following formula,

$$F = \frac{\text{Total amount of drug absorbed from rutin nano-complex } (A_{max} \text{ nano-complex})}{\text{Total amount of drug absorbed from pure rutin } (A_{max} \text{ pure rutin})} \times 100$$

$$F = \frac{(V_d \times K_{el} \times AUC_{0-\infty}) \text{ nano-complex}}{(V_d \times K_{el} \times AUC_{0-\infty}) \text{ pure rutin}} \times 100$$

Statistical Analysis

The data were expressed as mean ± standard error mean (SEM). For liver function test, *in vivo* antioxidant activity studies and pharmacokinetic studies, the statistical analysis was carried out using one-way analysis of variance (ANOVA) followed by Dunnett's and Student's t test. P values < 0.05 were considered as statistically significant.

RESULTS AND DISCUSSION

Formulation of Rutin Nano-complexes

In the preliminary studies, three different preparation methods of nano-complexes were screened for convenient nano-complex formation, namely solvent evaporation method, salting out method and lyophilisation method. In the qualitative solubility study of drug rutin, a good solubility

of rutin was obtained in DMF or DMSO in the form of clear rutin solution. Since DMSO has better safety profile (LD_{50} is 7.920 g/kg; oral dose in mice) compared to DMF (LD_{50} is 2.8 g/kg; oral dose in rat) (36), it was used as the main solvent in the study.

Maiti *et al.* reported that the solvent evaporation method is a possible method for the formation of a drug-phospholipid complex (18). Therefore, the solvent evaporation method was considered as one of the methods of the preparation of nano-complex using dioxane and methanol as a solvent mixture in the ratio of 7:3. However, in this solvent mixture, there was no clear rutin:EPC solution observed, which limited the formation of the nano-complex between rutin and EPC. It was supported by DSC studies, and the thermograms of rutin, EPC (Lipoid® E 80 S), a physical mixture of rutin:EPC (1:2) and rutin nano-complexes prepared by solvent evaporation, salting out and lyophilisation methods are given in Fig. 2. The thermogram of the nano-complex prepared by the solvent evaporation method (Fig. 2d) was found to be similar to the thermogram of the physical mixture of rutin:EPC in the ratio of 1:2 (Fig. 2c). DMSO could not be used in this method, though we obtained good solubility (qualitative) due to its high boiling point (189°C), as the phospholipids decompose at this high temperature (37). The DSC thermogram of the nano-complex prepared by the salting out method (Fig. 2e) suggested weak complex formation and decomposition upon the addition of n-hexane, dissolving the EPC and leaving the rutin precipitated.

Lyophilisation was the other method employed to formulate nano-complexes and found to be the method of choice as this method involves a simple procedure and fewer steps. Further, the evaporation and precipitation methods of development during the preparation were not observed, which were the major drawbacks associated with the other two methods, and therefore, lyophilisation was considered to be the single step preparation method, which resulted in a dry product (38). The DSC thermogram of the nano-complexes prepared by the lyophilisation method (Fig. 2f) also supported the complex formation (all the DSC thermograms obtained are discussed in the "RESULTS AND DISCUSSION" separately). By considering all these factors, the lyophilisation method was selected as the best possible method for the formulation of rutin nano-complexes.

For the selected nano-complex preparation method (lyophilisation), optimisation of different formulation variables was carried out. A suitable co-solvent for dissolving EPC was selected after proper screening of solvents like chloroform, acetone, methanol, ethanol and *t*-butyl alcohol apart from the main solvent, *i.e.* DMSO for rutin. EPC was required to be dissolved in a co-solvent without forming precipitation when it mixed with the solution of rutin dissolved in DMSO. From the visual observation, it was found that *t*-butyl alcohol and methanol formed a clear solution of EPC and rutin in DMSO without disturbing rutin's physical stability in DMSO solution. But due to the low freezing point of the methanol, it cannot be used in the lyophilisation process, since it has the sublimation step and it can only be possible if the solvent stays in frozen state. The high vapour pressure of the solvent is required to obtain the lyophilisation process with acceptable duration. DMSO alone is not a suitable solvent for lyophilisation since it has a high melting point of 19°C, but extremely low vapour pressure of 0.08 kPa at 25°C; hence, slow drying of the product was anticipated. The *t*-butyl alcohol has a high vapour pressure of

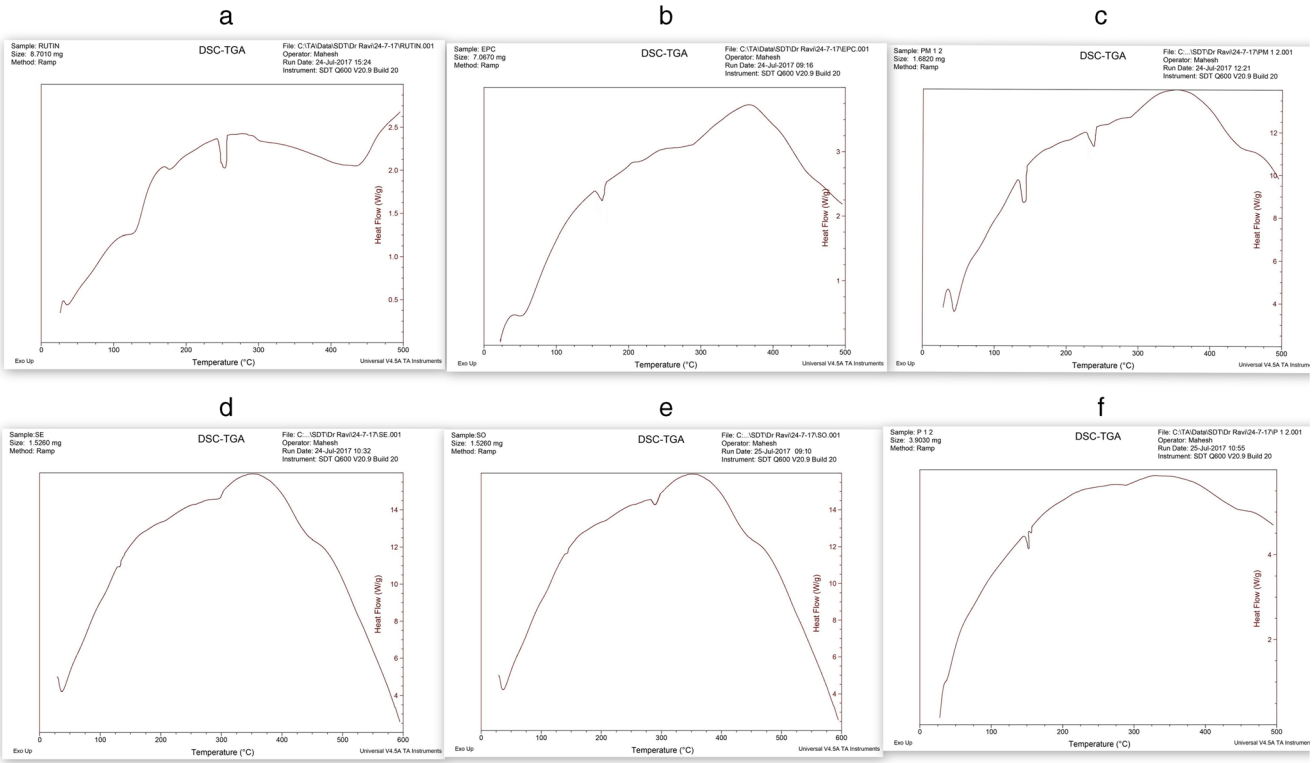

Fig. 2. DSC thermograms of rutin (**a**), EPC (**b**), physical mixture of rutin:EPC (1:2) (**c**) and rutin nano-complexes prepared by solvent evaporation (**d**), salting out (**e**) and lyophilisation (**f**) methods. DSC, differential scanning calorimetry; EPC, egg phosphatidylcholine

Table I. Composition and Characteristics of the Rutin Nano-complexes (F1–F4)

Formula	Rutin:EPC ratio	Particle size (nm)	Polydispersity index (PDI)	Zeta potential (mV)	Drug content (% *w*/*w*)
F1	1:1	274.2 ± 1.06	0.376 ± 0.02	− 34.7 ± 0.01	42.3 ± 0.04
F2	1:2	124.6 ± 0.01	0.495 ± 0.03	− 28.2 ± 0.12	54.7 ± 0.02
F3	1:3	173.6 ± 2.43	0.471 ± 0.01	− 23.7 ± 0.32	38.5 ± 0.01
F4	1:2 + 1% mannitol	240.7 ± 2.52	0.520 ± 0.02	− 15.4 ± 0.27	27.2 ± 0.02

Values are mean ± SEM ($n = 3$)
EPC, egg phosphatidylcholine; *PDI*, polydispersity index; *F*, formulation; *SEM*, standard error mean

4.1 kPa at 25°C and a high melting point of 24°C with low toxicity (39). Also, it was reported that subjecting *t*-butyl alcohol to the lyophilisation process leads to the formation of needle-like crystals with the larger surface area and high porosity which can facilitate the sublimation process. All these components conveyed the use of *t*-butyl alcohol as an ideal co-solvent (freeze-drying co-solvent) that could be eliminated thoroughly and rapidly by lyophilisation (40). Therefore, *t*-butyl alcohol was selected as an organic co-solvent to solubilise EPC, which is miscible with DMSO, in which rutin was dissolved as reported by Salazar *et al.* for the glibenclamide drug (41).

For the preliminary preparation of nano-complexes, drug:phospholipid was taken in a 1:2 ratio. Besides this, rutin nano-complexes were also formulated in 1:1 and 1:3 rutin:EPC ratio to give three nano-complex formulations

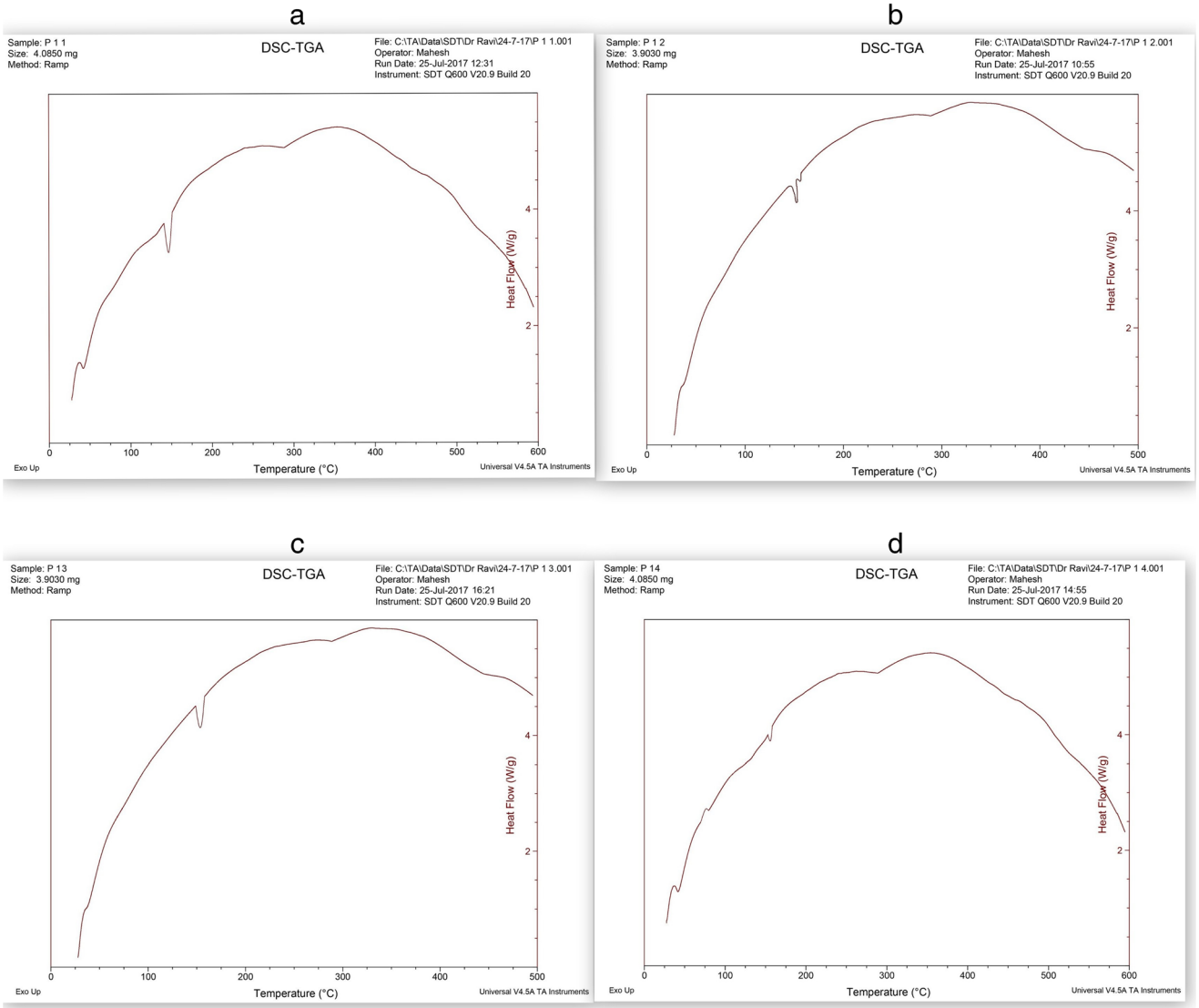

Fig. 3. DSC thermograms of rutin nano-complex formulations F1 (**a**), F2 (**b**), F3 (**c**) and F4 (**d**). DSC, differential scanning calorimetry; F, formulation

(F1, F2 and F3) as depicted in Table I. In one of the formulations (F4), the rutin:EPC ratio was kept at 1:2 and 1% *w/v* mannitol added as a cryoprotectant during the lyophilisation.

Evaluation of Rutin Nano-complexes

Thermal Response

Thermal analysis was carried out to investigate solid-state interactions, especially in complexes. DSC thermograms of rutin, EPC, physical mixture of rutin:EPC (1:2) and nano-complexes prepared by the solvent evaporation method, salting out method and lyophilisation method are given in Fig. 2. The thermogram of rutin (Fig. 2a) showed a sharp endothermal peak at 242°C corresponding to the melting point of rutin. A sharp endothermal peak was observed at 164.8°C in the thermogram of EPC (Fig. 2b), which may be due to the gel to liquid crystal state transition (20,36). As shown in the thermogram of the physical mixture of rutin:EPC (1:2) (Fig. 2c), the endothermal peaks of both rutin and EPC appeared but shifted towards the lower temperatures 233 and 138°C, respectively. As reported by Maiti *et al.*, drugs will dissolve in the molten phospholipids and partially form the phospholipid complexes on increase in temperature, which is in accordance with the preparation of the drug-phospholipid complexes by the melt out method (19). But the melt out method cannot be used in this study due to the high melting point of rutin (242°C), which leads to the decomposition of EPC (36). The DSC thermograms of the rutin nano-complex formulations (F1 to F4) are given in Fig. 3. It was observed in the DSC thermograms of all the formulations that the drug endothermal peaks disappeared, with an appearance of a new broad endothermal peak at 158°C, indicating the formation of a new complex peak near the EPC peak. These results are similar to the findings of Xu *et al.,* who reported the disappearance of luteolin endothermal peaks in the drug-phospholipid complex and the formation of a new complex peak due to the complex formation by interactions including hydrogen bonds or van der Waals forces (42). Further, the broad appearance of the peak does indicate that the complex is partially in an amorphous state.

Fourier Transform Infrared Spectroscopy

FTIR spectroscopic analysis was used to investigate the formation of nano-complex between rutin and EPC. The FTIR spectra of rutin, EPC, physical mixture 1:2 and nano-complex 1:2 obtained by the lyophilisation method (Fig. 4) were compared, and the characteristic peaks associated with specific functional groups and bonds of the molecule and their presence/ absence were noted by matching the absorption frequencies of the respective functional groups and bands (43). The changes were observed between the physical mixture and the nano-complex in the wave number ranging from 1231 to 942 cm^{-1} corresponding to the region of the EPC phosphate group. Broadening of the phenolic (–OH) band of rutin at 3637 cm^{-1} was also observed, which is a sign of H-bonding. The spectra of the physical mixture 1:2 and the nano-complex 1:2 obtained by the lyophilisation method showed an additive effect of rutin and EPC, in which the absorption peaks of rutin and EPC were still present at 1651 and 2852 cm^{-1}, respectively. These observations suggest that some weak physical interaction between the hydroxyl group of rutin and the phosphate group of EPC took place during the complex formation. This is in accordance with the findings of Xu *et al.*, who reported the formation of weak bonding between luteolin and phospholipid during complex formation (42). The FTIR spectra of the nano-complex formulations F1–F4 (Fig. 5) reflect the complex formation in all ratios which showed no significant difference in between.

Proton NMR (^{1}H-NMR)

The ^{1}H-NMR spectra of pure rutin, phospholipid (Lipoid® E 80 S) and rutin nano-complexes (F2) were recorded at 400 MHz frequency on (δ) scale, and ^{1}H

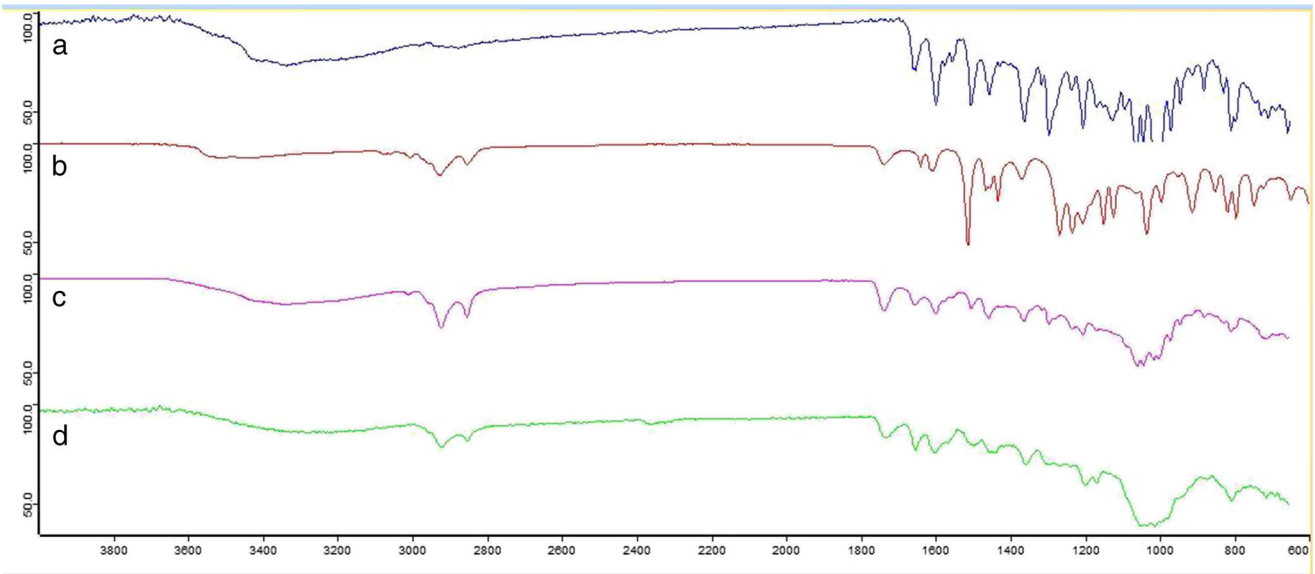

Fig. 4. IR spectra of rutin (**a**), EPC (**b**), physical mixture of rutin:EPC (1:2) (**c**) and rutin nano-complex prepared by lyophilisation method (**d**). IR, infrared; EPC, egg phosphatidylcholine

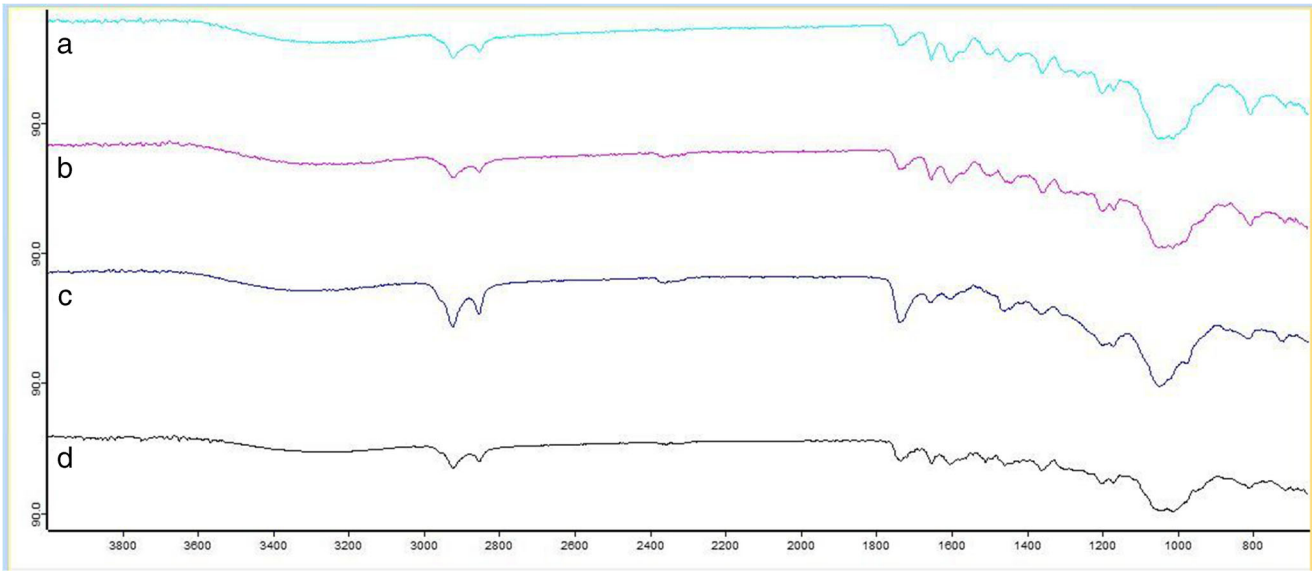

Fig. 5. IR spectra of rutin nano-complex formulations F1 (**a**), F2 (**b**), F3 (**c**) and F4 (**d**). IR, infrared; F, formulation

chemical shifts are reported in parts per million (ppm). The ^{1}H-NMR spectrum of pure rutin (Fig. 6a) exhibited the characteristic chemical shift values (δ, ppm; d6DMSO) as follows: δ 12.493 (s, 1H, OH at C5, 7), δ 10.775 (s, 2H, OH at C3′ and 4′), δ 9.586 (s, 1H, OH at C4″), δ 9.361 (d, J = 24.4 Hz, 4H, OH at C2, 3″ and 2, 3‴), δ 7.679–7.673 (d, J =

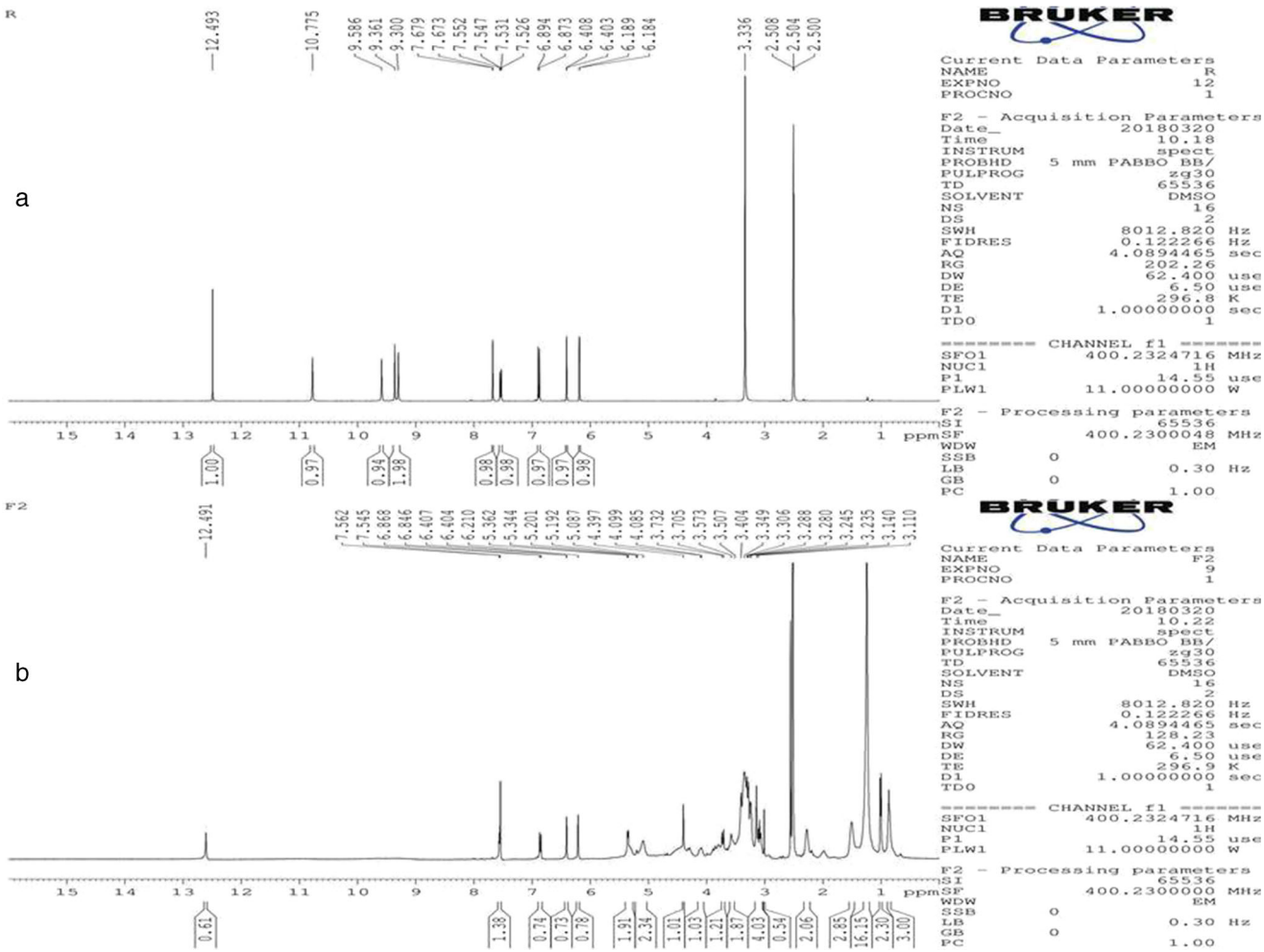

Fig. 6. ^{1}H-NMR spectra of rutin (**a**) and rutin nano-complex (**b**) in DMSO. ^{1}H-NMR, proton nuclear magnetic resonance; DMSO, dimethyl sulphoxide

2.4 Hz, 2H at C2′ and 6′-H), δ 7.547–7.526 (dd, J = 2.0 Hz, 4H, H at C2, 3″ and 2, 3‴), δ 6.894–6.873 (d, 1H at C-5′), δ 6.408–6.403 (d, 1H at C8), δ 6.189–6.184 (d, 1H at C6-H), δ 3.336 (s, 2H, H at CH2 bridge) and δ 2.508–2.500 (t, J = 1.6 Hz, 2H, H at C4″). The δ values obtained were in agreement with the values reported in the literature (44). The ^{1}H-NMR spectrum of Lipoid® E 80 S exhibited the characteristic chemical shift values (δ, ppm; d6DMSO) as follows: δ 5.331 (2H, t, J = 3.2), δ 3.342 (4H, s, –OCH2), δ 2.516 (3H, s, CH3), δ 2.288 (t, J = 3.2, 16H), δ 2.050 (d, J = 6.4 Hz, 8H), δ 2.018 (d, J = 6.8, 1H, CH2), δ 1.510 (s, 23H) and δ 1.270 (s, 3H), and the ^{1}H-NMR spectrum of the prepared rutin nano-complex (Fig. 6b) showed the characteristic chemical shift values at δ 12.491 (s, 1H, OH at C5,7), δ7.562–7.545 (d, J = 6.8 Hz, 2H, H at C2'and 6'-H), δ6.868–6.846 (d, J = 8.8 Hz, 1H at C¬5′), δ6.407–6.404 (d, J = 1.2 Hz, 1H at C8), δ6.210 (s, 1H at C6-H), δ5.362–5.344 (d, J = 7.2 Hz, 1H Glu), δ 5.201–5.192 (d, J = 3.6 Hz, 2H Phos), δ 5.087(s, 1H Rham), δ 4.397 (s, 1H, CH, Rham), δ 4.099–4.085 (d, J = 5.6 Hz, H at Glu), δ 3.732–3.705 (d, J = 10.8 Hz, H at CH2, Glu), δ 3.573–3.110 (s, d, dd, H of Phos), δ 3.349 (s, 3H, H at CH3) and δ 3.306 (s, 2H, H at CH2 bridge). In ^{1}H NMR, proton peaks at δ 9.5 for H-4′ and δ 10.7 for H-7′-OH are missing in the rutin nano-complex formulation indicating the interaction of phospholipid with the negative oxygen of labile –OH group. The downfield shift of H-5 proton of rutin in rutin nano-complex formulation at δ 12.4 indicated its intramolecular hydrogen bonding with the C-4 ketonic function. This confirmed the formation of molecular complexes of rutin with phospholipid (45).

X-ray Powder Diffractometry

The X-ray crystallography technique is used to determine the molecular crystallinity of the rutin nano-complex. The X-ray diffractograms of pure rutin, EPC and rutin nano-complex (F2) are shown in Fig. 7. The X-ray diffractogram of pure rutin (Fig. 7a) showed the intense and sharp diffraction peaks of crystallinity at $2\theta = 12.0769°$, 15.5618°, 23.4592° and 27.0049°C which proves that rutin is crystalline in nature. The X-ray diffractogram of EPC (Lipoid® E 80 S) (Fig. 7b) showed a single, relatively broad diffraction peak at $2\theta = 19.567°$. The absorbance of any additional, well-defined, sharp crystalline peaks in Lipoid® E 80 S diffractogram indicated the amorphous nature of the phospholipid. The X-ray diffractogram of the rutin nano-complex (Fig. 7c) exhibited a single broad peak at $2\theta = 20.9873°$. The disappearance and reduction in the intensity of large diffraction peaks of pure rutin suggested that rutin in the rutin nano-complex may be molecularly dispersed in the phospholipid matrix and formed an amorphous form. The reduction in

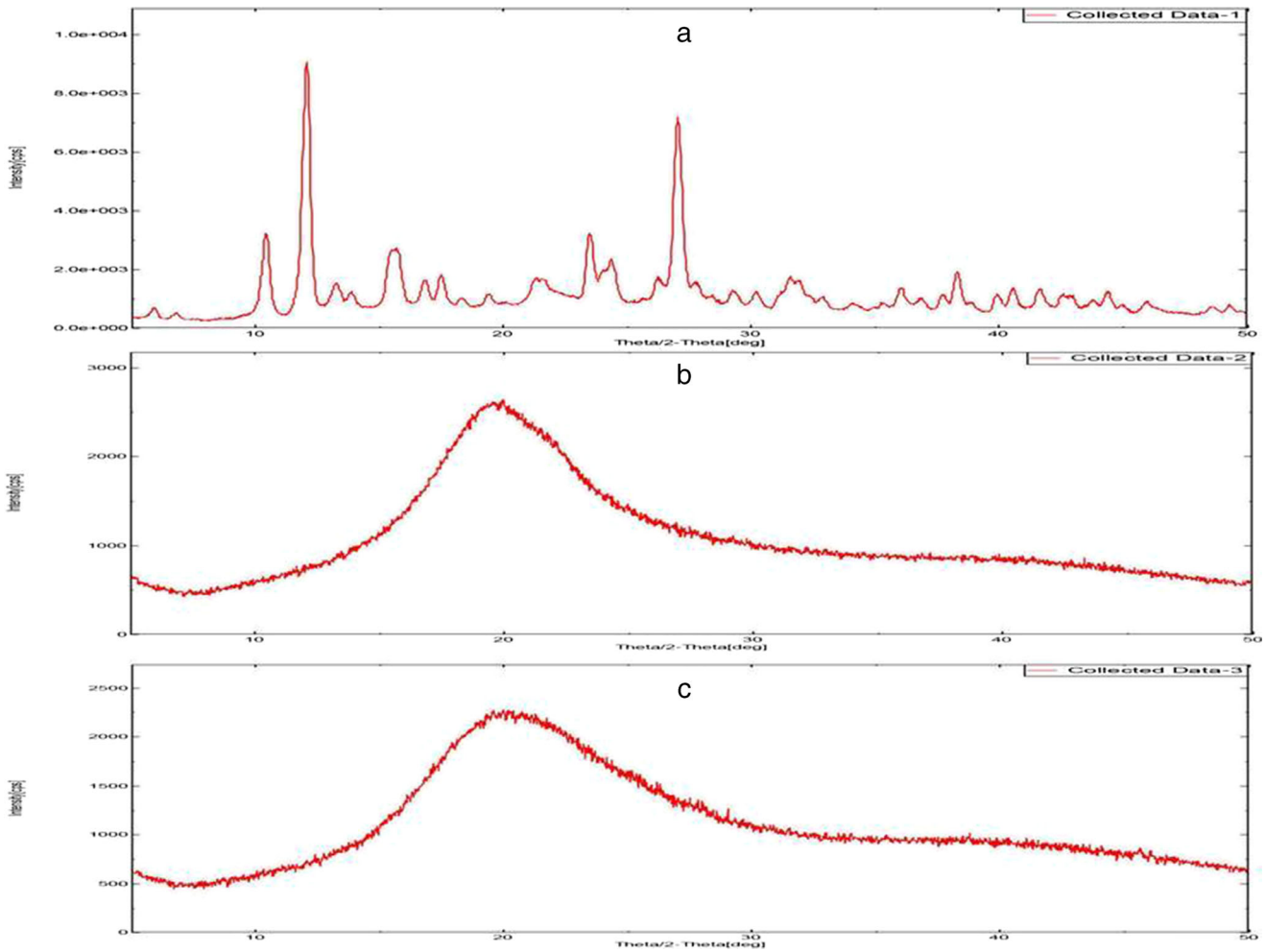

Fig. 7. X-ray diffractograms of pure rutin (**a**), EPC (**b**) and rutin nano-complex (**c**). EPC, egg phosphatidylcholine

crystallinity of rutin in the rutin nano-complex formulation may also be a reason for its increased solubility as it is a known fact that amorphous substances are more soluble in nature compared to their crystalline forms.

Particle Size Analysis and Zeta Potential

The formulated rutin nano-complexes were characterised for particle size, zeta potential and PDI (Table I). The nano-complexes diluted with distilled water are expected to possess a negative charge due to the phosphate group of the EPC in the surrounding water with a neutral pH value (38). F1 formulation with 1:1 ratio of rutin:EPC showed particle size of 274.2 nm, zeta potential −34.7 mV and PDI 0.376. The higher particle size and increased negativity in the surface charge of F1 formulation than F2 may be due to the presence of free rutin and EPC due to weak bonding. In F2 formulation, reduction in particle size (124.6 nm) was observed with an adequate zeta potential (−28.2 mV) and PDI (0.495) compared to F1 formulation, which may be due to physical bonding of all rutin molecules to the polar heads of EPC, suggesting that the 1:2 ratio of rutin:EPC is optimum to form nano-complexes. Results of F3 formulation suggested further increase in the rutin:EPC ratio from the proposed optimum ratio which leads to an increase in particle size (173.6 nm) and a decrease in zeta potential (−23.7 mV) with PDI of 0.471. This might be due to the aggregation of excess EPC molecules that have complexed with rutin molecules resulting in higher particle size and lower surface charge. The F4 formulation in which 1% *w/v* mannitol was added as cryoprotectant showed higher particle size (240 nm) and PDI (0.520) with low zeta potential value (−15.4 mV) in comparison with F2 formulation without cryoprotectant. This is due to the crystal nature of mannitol and the formation of the eutectic composition with ice, which can cause phase separation in the cryo-concentrated portion of the frozen nano-complex. The lower zeta potential value might be due to the shielding of the negativity of EPC by mannitol molecules. Further, the lower zeta potential value also indicated decreased stability. Homogenisation or extrusion may not be an appropriate method to reduce the PDI in the nano-complex formulations as it may lead to the decomposition of the rutin:EPC complex (46).

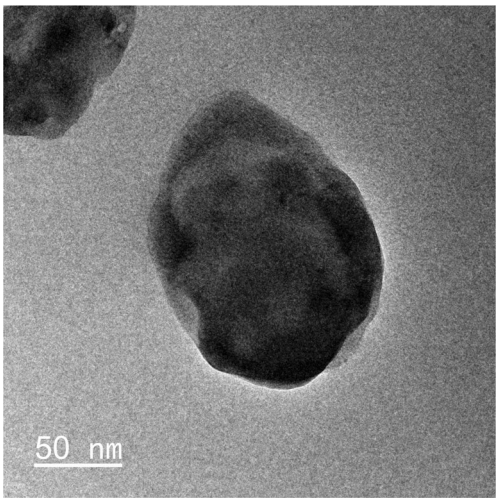

Fig. 9. TEM image of rutin nano-complex with 20-fold dilution in distilled water. TEM, transmission electron microscopy

Surface Morphology

The SEM images of the pure drug rutin (Fig. 8a) and selected rutin nano-complex formulation (F2) (Fig. 8b) revealed that the crystalline drug rutin is converted into a nano-complex which exhibited a fluffy, porous and rough surface, which might have improved the solubility and dissolution compared to pure rutin. The TEM image (Fig. 9) of the selected rutin nano-complex formulation (F2) showed well-formed, discrete vesicles as the rutin nano-complexes are formed by combining the polar head of the EPC and the polar functional group of rutin. When nano-complexes swirled in distilled water, they formed vesicular nanostructures with no evidence of aggregation or decomposition.

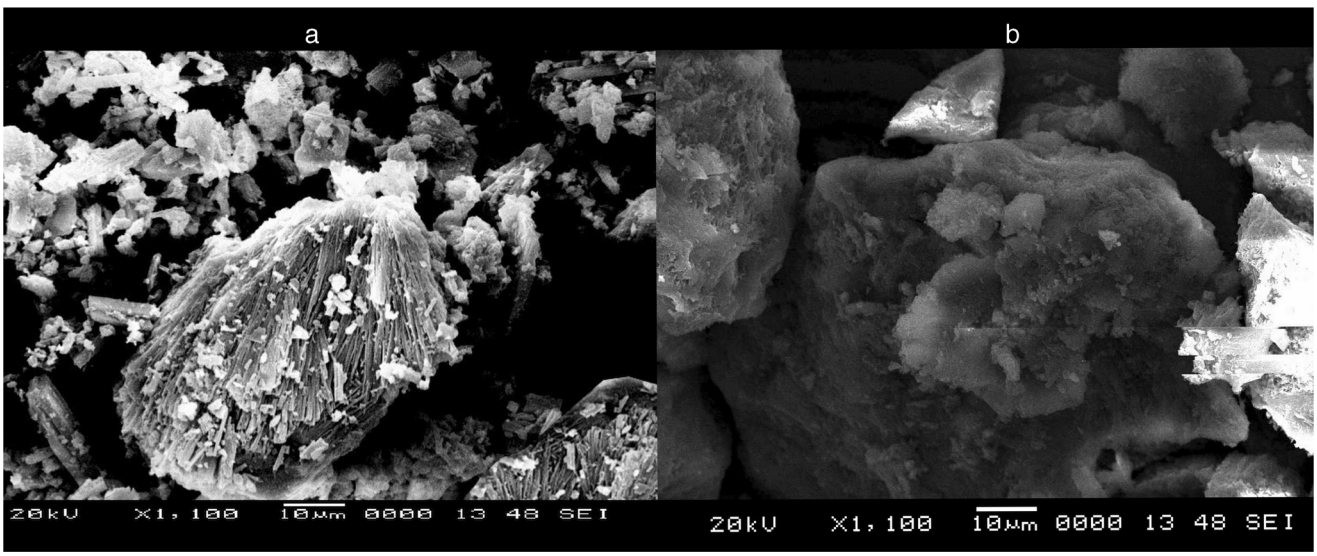

Fig. 8. SEM image of pure rutin (**a**) and rutin nano-complex (**b**) (×1100). SEM, scanning electron microscopy

Drug Content

The results of drug content estimation by HPLC are summarised in Table I. The F2 formulation showed maximum drug content of 54.7 ± 0.02% *w/w*.

In Vitro Stability Study

In vitro stability study of the selected formulation (F2) was carried out to predict the physical stability of the rutin nano-complexes after intake into the GIT, by observing the changes in physicochemical properties like particle size, zeta potential and PDI and physical factors like aggregation and precipitation. The stability study of F2 formulation after 2 h in SGF (pH 1.2) showed reduced particle size upon incubation from 106.7 ± 2.56 to 88.95 ± 1.73 nm. Insignificant variations were observed after 2 h for PDI (0.96 ± 0.01) and zeta potential (+ 23.1 ± 0.23 mV) compared to initial PDI (0.89 ± 0.03 and zeta potential (+ 15.4 ± 0.18 mV). In SIF (pH 7.4), particle size reduced from 301.4 ± 2.86 to 269.9 ± 2.12 nm after incubation, and insignificant changes were observed in initial PDI (0.53 ± 0.002) and zeta potential (− 14.7 ± 1.12 mV) compared to the PDI (0.61 ± 0.01) and zeta potential (− 9.66 ± 1.36 mV) after 6 h. Aggregation or precipitation was not seen either in SGF or SIF fluid. These results indicated the stability of the rutin nano-complexes after incubation in different pH media. A positive charge (+ 23.1 ± 0.23 mV) in the acidic condition (pH 1.2), a negative charge in water (− 28.2 ± 0.12) and a lower negative charge in pH 7.4 phosphate buffer (− 9.66 ± 1.36 mV) were observed due to the dual charge of EPC. The acidic medium neutralises the phosphate oxygen negativity allowing positive charge to predominate. Higher pH (water and SIF) neutralises choline positive charge leading to negatively charged vesicles. These results suggest that the shelf life stability of the rutin nano-complex does not require high repulsion force. Results of the *in vitro* stability study are given in Table II.

Solubility Studies

Rutin is hydrophobic in nature and poorly soluble in water. Its poor solubility leads to poor absorption and poor permeation across the enterocytes of the intestine leading to reduced bioavailability. The aqueous solubility of rutin was observed ~ 1.7 μg/mL and relatively higher solubility was observed in n-octanol (~ 44.58 μg/mL) which indicated that rutin is lipophilic in nature. The prepared rutin nano-complex (F2) showed a highly significant increase (over 25-fold) in the aqueous solubility compared to pure rutin ($P < 0.001$). This may be due to the amphiphilic, amorphous and porous characteristic of the complex compared to the molecular crystallinity of pure rutin, which is supported by SEM and XRD study results. The partition coefficient of pure rutin and rutin nano-complex (F2) in n-octanol/phosphate buffer pH 7.4 was found to be 2.59 ± 0.539 and 0.67 ± 0.073, respectively. The results of the solubility study of rutin and rutin nano-complex formulation (F2) in water and n-octanol are depicted in Table III.

In Vitro Drug Release Study

In vitro drug release study was conducted to investigate the rapidity of rutin release from the rutin nano-complexes. The output obtained by the dialysis method helps to predict a correlation with *in vivo* drug release. *In vitro* drug release profile of pure rutin and rutin:EPC complex (F1–F3) in acidic buffer pH 1.2 (up to 2 h) and phosphate buffer pH 7.4 (2–24 h) is shown in Fig. 10. The pure rutin showed 18.2% drug release at the end of 2 h in acidic pH 1.2 and 54.3% drug release at the end of 24 h in phosphate buffer pH 7.4. Unlike pure rutin, the rutin nano-complex formulations (F1–F3) showed high drug release at the end of 24 h, but in acidic pH, the drug release was less than that of the pure rutin. The F2 formulation showed better drug release of 74.4% at the end of 24 h. The results showed that the improved release of rutin from the rutin nano-complex may be because of increased solubility and wettability of the nano-complex due to its amorphous nature compared to pure rutin which is crystalline in nature. The fluffy, porous and rough surface of the nano-complex also helped to improve the dissolution of the nano-complex, which was also supported by the SEM and solubility studies. Higuchi's plot of the rutin nano-complex formulations was found to be linear and confirmed diffusion-controlled drug release. The sustained release of rutin occurs in two steps. First, in aqueous media, rutin dissociates from the complex, and in the second step, the dissociated free rutin will diffuse out of the phospholipid matrix; hence, the rutin nano-complex enhances the rate and extent of rutin release compared to pure rutin (47).

In Vitro Antioxidant Activity

In vitro antioxidant activity of pure rutin and the rutin nano-complex (F2) was evaluated as free radical scavenging activity (% of DPPH scavenged). The % inhibition of DPPH by pure rutin and rutin nano-complex was compared with the % inhibition of DPPH by standard (ascorbic acid). The % inhibition of DPPH at 50 μg/mL concentration by ascorbic

Table II. *In Vitro* Stability of Rutin Nano-complex in SGF and SIF Without Enzymes

Media	Time interval	Particle size (nm)	Polydispersity index (PDI)	Zeta potential (mV)
SGF	Zero time	106.7 ± 2.56	0.89 ± 0.03	+ 15.4 ± 0.18
	2 h	88.95 ± 1.73	0.96 ± 0.01	+ 23.1 ± 0.23
SIF	Zero time	301.4 ± 2.86	0.53 ± 0.02	− 14.7 ± 1.12
	6 h	269.9 ± 2.12	0.61 ± 0.01	− 9.66 ± 1.36

Values are mean ± SEM ($n = 3$)
SGF, simulated gastric fluid; *SIF*, simulated intestinal fluid; *SEM*, standard error mean

Table III. Solubility of Pure Rutin and Rutin Nano-complex in Water and N-octanol at 37°C

Medium	Solubility (μg/mL)	
	Pure rutin	Rutin nano-complex
Water	1.76 ± 0.264	44.58 ± 0.248
N-octanol	126.18 ± 2.143	210.86 ± 1.216

Values are mean ± SEM ($n = 3$)
SEM, standard error mean

acid, pure rutin and rutin nano-complex (F2) was found to be 91.75 ± 1.46, 29.30 ± 1.58 and 44.53 ± 1.98%, respectively, and the results are depicted in Fig. 11. The results revealed the significant free radical scavenging activity of rutin in nano-complex, which can be attributed to the increased ability of the rutin to donate hydrogen ions and reducing DPPH radical to corresponding hydrazine (48).

In Vivo Hepatoprotective (Liver Function Test) and Antioxidant Activity Studies

Serum Analysis

The liver has the function to detoxify toxic substances and synthesise useful biomolecules as a key organ of metabolism and excretion. Hepatotoxicants such as bacterial metabolites, fungal products, viruses, environmental pollutants, minerals and chemotherapeutic agents induce liver damage. Liver diseases are the major ones among the various health problems, including liver cirrhosis, fibrosis, hepatocellular carcinoma and hepatitis, which appears to be the most serious. Hepatotoxins, such as ethanol, acetaminophen and CCl_4, induced liver injury, which is characterised by varying degrees of hepatocyte degeneration and cell death. CCl_4 decreases the activities of antioxidant enzymes and enhances the formation of free radicals, which cause lipid peroxidation of cellular and organelle membranes, and has been widely used as a hepatotoxic agent. CCl_4 induces the increase in serum SGOT and SGPT levels due to the cell membrane and mitochondrial damage of liver cells. CCl_4 is reported to be metabolised by the hepatic cytochrome P-450 enzymes into reactive oxygen species (ROS), and the covalent binding of these metabolites (trichloromethyl free radicals) to cellular macromolecules (*e.g.* lipids, proteins, nucleic acids) is considered to be the first step in a chain of events that eventually lead to membrane lipid oxidation and ultimately to the death of the cell (49,50). Liver injury can be confirmed when there is a rise in either (i) ALT level more than three times of the upper limit of normal (ULN), (ii) SALP level more than twice the ULN or (iii) total bilirubin level more than twice the ULN when associated with the increased ALT or ALP (51). In the present study, after inducing the hepatic damage by CCl_4 intoxication, the rat serum was analysed for the marker enzymes and a significant rise in SGPT, SGOT, SALP and also serum bilirubin levels was observed. In the CCl_4-intoxicated group, the SGPT level was increased by 3 times, the SGOT level increased by more than 2.5 times, the SALP by more than 1.5 times and total bilirubin level was increased by more than 2 times than that of the normal group, which confirmed the hepatic damage caused by CCl_4. It was evident that pre-treatment with the rutin nano-complex better restored the normal enzyme levels compared to pure rutin at the same dose levels (100 and 200 mg/kg). The results of the liver function tests are depicted in Table IV. The same group of animals showed fewer variations despite having difference in their body weight due to several reasons, such as drug dose was calculated based on the body weight of individual rats and the living environment was continually adapting to seasonal demands of survival and also the reproduction.

Rutin is a powerful free radical scavenger; thus, it can shield the liver from the adverse effects of CCl_4 (52). The results of the assay of marker enzymes of antioxidant studies in normal, CCl_4-intoxicated, pure rutin-treated and rutin nano-complex (F2)-treated rat groups are depicted in Table V. Compared to the normal group, levels of GSH, GPx, GST, GRD, SOD and CAT significantly reduced ($P < 0.01$). It was also observed that the levels of these

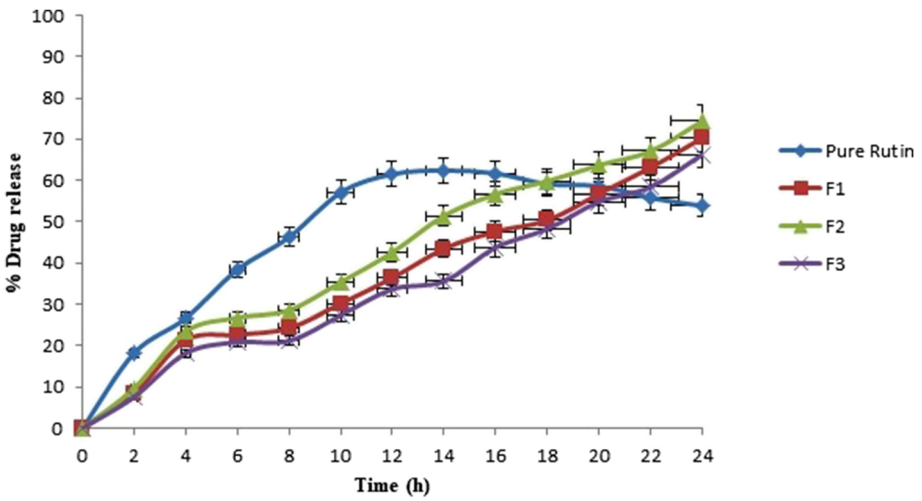

Fig. 10. *In vitro* drug release profile of pure rutin and rutin nano-complex (F1–F3) in acidic buffer pH 1.2 (up to 2 h) and phosphate buffer pH 7.4 (2–24 h). Values are mean ± SEM ($n = 3$). *$P < 0.001$ (significant with respect to free rutin). EPC, egg phosphatidylcholine; SEM, standard error mean; h, hour; F, formulation

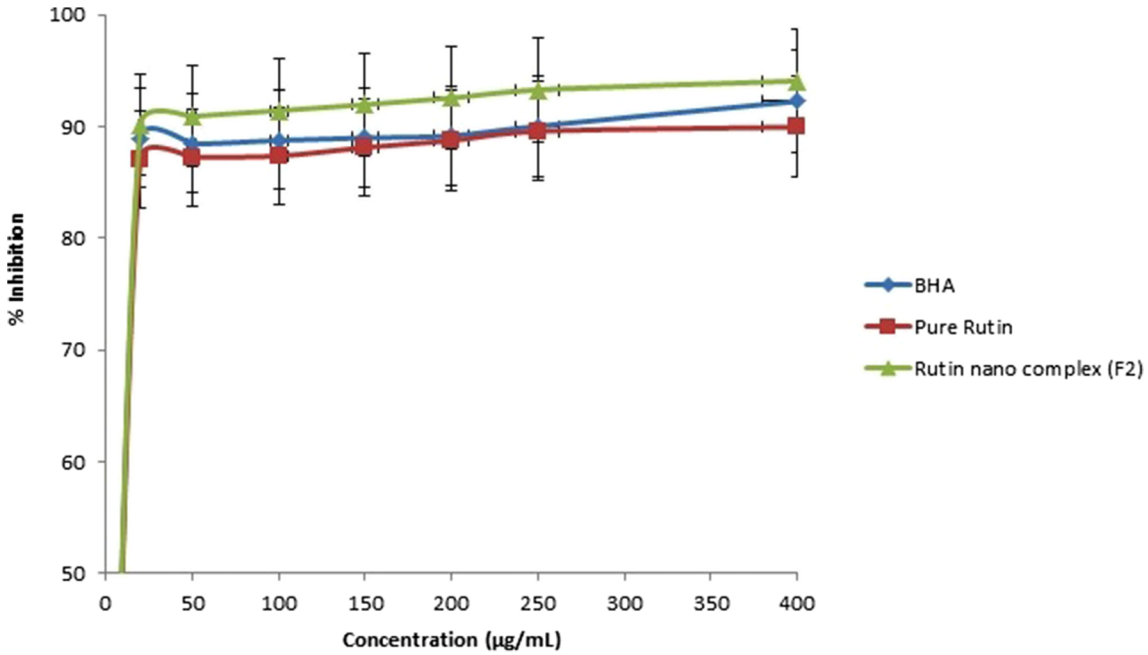

Fig. 11. % inhibition of DPPH by standard (ascorbic acid), pure rutin and rutin nano-complex (F2). Values are mean ± SEM ($n = 3$). DPPH, 2,2-diphenyl-1-picrylhydrazyl; SEM, standard error mean; F, formulation

enzymes were better restored in the rutin nano-complex (equivalent to 100 and 200 mg/kg of rutin)-treated groups compared to pure rutin-treated groups at the same dose levels. This result marginally differed from the findings of Maiti *et al.*, who reported that treatment with free quercetin drug at 10 mg/kg did not produce any significant result in the SOD level (22). The TBARS level was increased significantly ($P < 0.05$) in the CCl_4-intoxicated rat group compared to the normal group. The rutin nano-complex (equivalent to 100 and 200 mg/kg)-treated groups showed a better increase in TBARS levels towards the normal compared to animal groups treated with pure rutin at the same dose levels (Fig. 12). Trichloromethyl radical produced by the action of cytochrome P-450 in CCl_4-induced hepatotoxicity initiates the cascade of free radical reactions which increases the lipid peroxidation and reduction in hepatic enzyme actions (53–55). The rutin nano-complex at the dose equivalent to 200 mg/kg of rutin better restored the normal enzyme levels which in turn enhanced the therapeutic efficacy of rutin towards hepatic protection. The reason behind this is the formation of catecholic (o-diphenolic) metabolites (3,4-dihydroxyphenylacetic acid and 3,4-dihydroxybenzoic acid) from rutin which is able to scavenge two free radicals, in two successive $1H^+/1e^-$ processes (56).

Histopathological Studies

Photomicrographs of the histopathological study of rat liver sections of all rat groups are shown in Fig. 13. The normal control group of animal liver sections showed clear nucleus, nucleolus, veins and cytoplasm (Fig. 13a), but the liver tissues of the CCl_4-intoxicated rat groups showed visible damage and degeneration of parenchyma cells, degeneration of liver fatty tissue and damage of the central lobular region (Fig. 13b). Rutin nano-complex (equivalent to 100 and 200 mg/kg of rutin) pre-treatment (Fig. 13f) better restored the altered histological changes induced by CCl_4 compared to the same dose of pure rutin pre-treatment. Restoration of the

Table IV. Liver Function Test After CCl_4-Induced Hepatotoxicity in Rats on the 8th Day ($n = 6$)

Parameters	Group I Normal	Group II CCL_4 treated	Group III CCL_4 + rutin (100 mg/kg)	Group IV CCL_4 + rutin (200 mg/kg)	Group V CCL_4 + rutin nano-complex (~ 100 mg/kg)	Group VI CCL_4 + rutin nano-complex (~ 200 mg/kg)
SGPT (U/L)	40.98 ± 2.49**	120.73 ± 5.54	93.40 ± 2.43**	78.71 ± 3.16*	81.75 ± 1.87**	63.68 ± 2.27**
SGOT (U/L)	36.18 ± 3.40**	94.26 ± 4.62	81.25 ± 4.21*	64.92 ± 3.36	70.64 ± 1.85**	48.23 ± 1.67**
SALP (U/L)	146.81 ± 3.84**	224.79 ± 2.46	196.43 ± 2.12*	169.58 ± 2.87	172.49 ± 1.86**	151.25 ± 1.92**
Total bilirubin (mg/dL)	0.58 ± 0.02**	1.24 ± 0.01	0.96 ± 0.01**	0.76 ± 0.01*	0.87 ± 0.02**	0.68 ± 0.01**

Values are mean ± SEM
SGOT, serum glutamate oxaloacetate transaminase; *SGPT*, serum glutamate pyruvate transaminase; *SALP*, serum alkaline phosphatase; *CCl_4*, chloroform; *SEM*, standard error mean
*$P < 0.05$, **$P < 0.01$ (significant with respect to the CCl_4-treated group)

Table V. Effect of Rutin Nano-complex on the Levels of GSH, GPx, GST and GRD in CCl_4-Intoxicated Rats on Day 8 ($n = 6$)

Parameters	GSH (nmol/mg protein)	GPx (nmol of NADPH oxidised/ min/mg protein)	GST (nmol of CDNB conjugate formed/min/mg protein)	GRD (nmol of oxidised glutathione [GSSG] utilised/min/mg protein)	SOD (U/mg protein)	CAT (U/mg protein)
Group I Normal	46.23 ± 4.48**	324.47 ± 6.73**	292.71 ± 5.84**	20.27 ± 2.86**	7.28 ± 0.03**	204.76 ± 3.46**
Group II CCL_4 treated	20.18 ± 2.59	186.32 ± 4.82	156.14 ± 6.69	8.39 ± 1.92	4.37 ± 0.02	96.57 ± 2.59
Group III CCL_4 + rutin (100 mg/kg)	31.29 ± 2.21*	240.09 ± 4.36**	210.55 ± 4.28	12.45 ± 0.81	4.93 ± 0.14	136.64 ± 4.95*
Group IV CCL_4 + rutin (200 mg/kg)	38.64 ± 3.86**	286.74 ± 2.87**	246.92 ± 3.67**	16.23 ± 1.17**	5.36 ± 0.04**	172.27 ± 3.83**
Group V CCL_4 + rutin nano-complex (eq to 100 mg/kg)	36.57 ± 2.97**	269.38 ± 4.25**	234.47 ± 4.96*	15.39 ± 1.24**	6.24 ± 0.10**	164.49 ± 3.52**
Group VI CCL_4 + rutin nano complex (eq. to 200 mg/kg)	44.29 ± 3.81**	310.19 ± 2.51**	281.94 ± 5.37**	18.94 ± 1.02**	6.85 ± 0.03**	197.44 ± 2.87**

Values are mean ± SEM
GSH, glutathione; *GPx*, glutathione peroxidase; *GST*, glutathione S transferase; *GRD*, glutathione reductase; *SOD*, superoxide dismutase; *CAT*, catalase; *CCl_4*, chloroform; *SEM*, standard error mean
*$P < 0.05$, **$P < 0.01$ (significant with respect to the CCl_4-treated group)

normal anatomy of the hepatic cellular structure by pure rutin and the rutin nano-complexes can be imputed to the strong antioxidant activity properties of rutin (57).

Oral Bioavailability Studies

The Concentration of Rutin in Rat Serum

There are many intrinsic factors that affect the oral absorption of a drug and these can be studied by performing *in vivo* studies; hence, *in vivo* bioavailability studies were carried out to determine the oral absorption of the rutin nano-complex compared to pure rutin. The mean plasma concentration-time curves of pure rutin and the rutin nano-complex in the serum of rats treated with pure rutin (100 mg/kg, p.o.) and the rutin nano-complex (~ 100 mg/kg of rutin, p.o.) are depicted in Fig. 14. Pure rutin attained 6.47 ± 0.12 μg/mL maximum serum concentration at 4.0 h, and the rutin nano-complex showed maximum serum concentration of 9.95 ± 0.57 μg/mL at 6.0 h and the serum concentration was also maintained for a longer period of time.

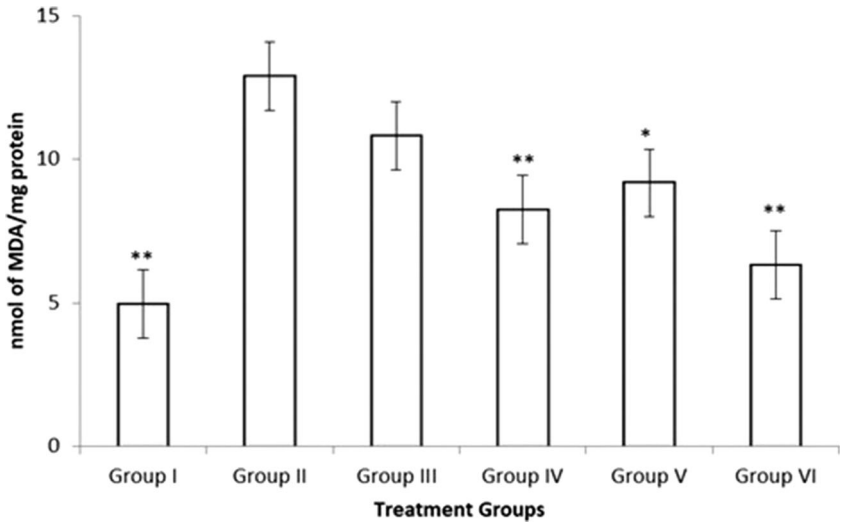

Fig. 12. Effect of rutin nano-complex on TBARS. Group I: normal, group II: CCL_4 treated, group III: CCl_4 + rutin (100 mg/kg), group IV: CCl_4 + rutin (200 mg/kg), group V: CCl_4 + rutin nano-complex (~ 100 mg/kg), group VI: CCl_4 + rutin nano-complex (~ 200 mg/kg). Values are mean ± SEM ($n = 6$). *$P < 0.05$, **$P < 0.01$ (significant with respect to the CCl_4-treated group). TBARS, thiobarbituric acid reactive substance; CCl_4, chloroform; SEM, standard error mean

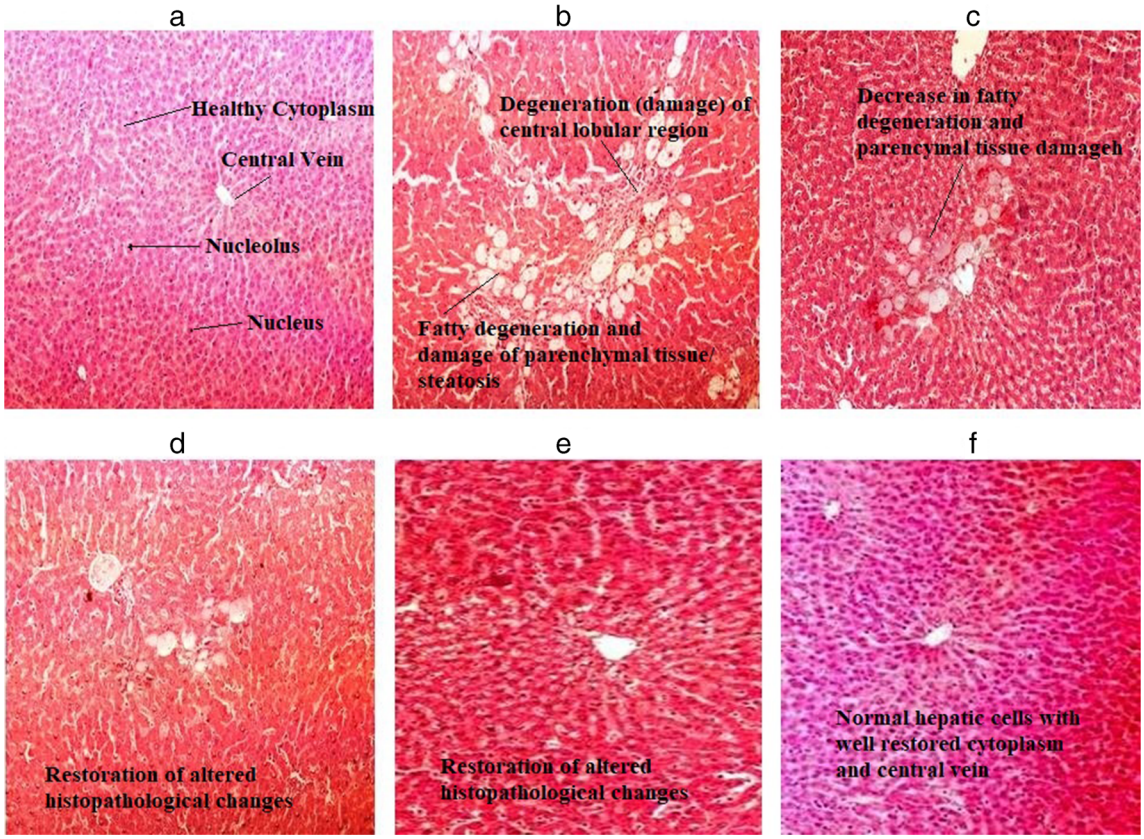

Fig. 13. Photomicrographs of **a** normal rat liver section, **b** CCl_4-intoxicated rat liver section, **c** pure rutin (100 mg/kg)-treated rat liver section, **d** pure rutin (200 mg/kg)-treated rat liver section, **e** rutin nano-complex (~100 mg/kg)-treated rat liver section and **f** rutin nano-complex (~ 200 mg/kg)-treated rat liver section. CCl_4, chloroform; SEM, standard error mean

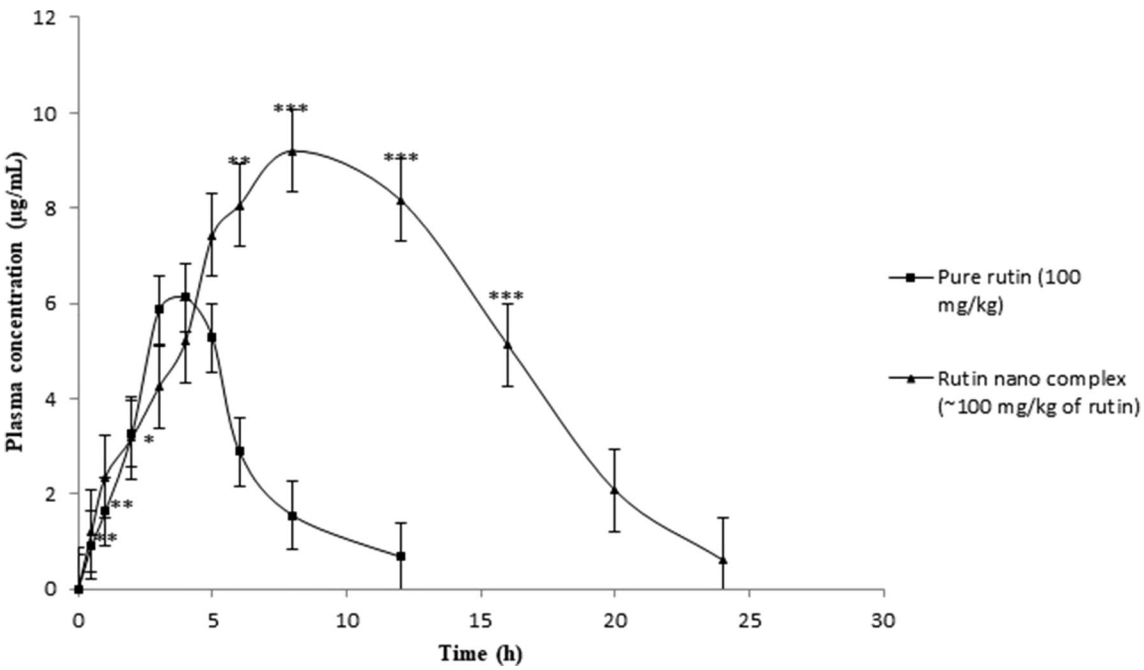

Fig. 14. Mean plasma concentration-time profile of rutin (100 mg/kg, p.o.) and rutin nano-complex (~ 100 mg/kg of rutin, p.o.). Values are mean ± SEM ($n = 6$). *$P < 0.05$, **$P < 0.001$ and ***$P < 0.0001$ (significant with respect to the pure rutin-treated group). SEM, standard error mean

Table VI. Pharmacokinetic Parameters of Pure Rutin (100 mg/kg, p.o.) and Rutin Nano-complex (~ 100 mg/kg of Rutin, p.o.) in Rats

Pharmacokinetic parameters	Pure rutin	Rutin nano-complex
C_{max} (μg mL^{-1})	6.47 ± 0.12	9.95 ± 0.57
T_{max} (h)	4.0	6.0
AUC_{0-t} (μg mL^{-1} h)	39.51 ± 1.16	115.61 ± 4.69
$AUC_{0-\infty}$ (mL^{-1} h)	40.64 ± 2.76	152.34 ± 6.48
Elimination half-life ($t_{1/2el}$) (h)	1.97 ± 0.10	3.49 ± 0.27
Elimination rate constant (K_{el}) (h^{-1})	0.51 ± 0.004	0.17 ± 0.001
Clearance (Cl) (L h^{-1})	0.56 ± 0.002	0.14 ± 0.002
Volume of distribution (V_d) (L)	1.42 ± 0.26	0.98 ± 0.01

Values are mean ± SEM ($n = 3$)
C_{max}, maximum plasma concentration; T_{max}, time required to reach maximum concentration; *AUC*, area under curve; *SEM*, standard error mean

Pharmacokinetic Parameters

The pharmacokinetic parameters calculated from the plasma concentration-time curve, using the computer software WinNonlin®, are shown in Table VI. C_{max}, T_{max} and elimination half-life values were increased in the serum of animals treated with rutin nano-complex compared to the animals treated with pure rutin. Elimination rate constant, clearance and volume of distribution values were decreased in the nano-complex-treated rat serum. The rutin nano-complex remained for an extended period of time in the body with a high relative bioavailability of 86.23%. The reason for the significant enhancement in the relative bioavailability of the rutin nano-complex is due to phospholipid as an essential cell membrane component retained the fluidity of the cell membrane and also enhances the significantly aqueous solubility of the nano-complex compared to pure rutin. Phospholipids also increase the rate and extent of rutin absorption into the intestinal mucosa and are possibly the reason for the increase in relative bioavailability (58). Our results were compatible with Freag *et al.*, who developed the self-assembled phospholipid-based phytosomal nanocarriers of celastrol as promising platforms for improving oral bioavailability (59). In the present study, the oral bioavailability of rutin was enhanced, and this may be great evidence which showcases the potentiality of this technology to enhance the efficiency of many phytoconstituents with high therapeutic benefits but has some lacunae regarding oral absorption and bioavailability. The safety profile of the formulation is an added advantage as regulatory aspects are considered. However, further investigations in the light of *in vitro-in vivo* correlation (IVIVC) and clinical trials will facilitate their way to the market.

CONCLUSION

In this study, rutin nano-complexes were successfully developed by the lyophilisation method. The physicochemical characteristics of pure rutin have changed significantly after complexing it with EPC, such as lower particle size, adequate zeta potential and PDI, improved solubility due to the decrease in molecular crystallinity and increased stability. The study also proved the better therapeutic effect of the rutin nano-complex with promising oral bioavailability in rats for prolonged time compared to pure rutin. Established results revealed that the complexation of rutin with EPC may be considered promising in order to boost the absorption and oral bioavailability of rutin facilitating its clinical use as a hepatoprotective agent.

ACKNOWLEDGMENTS

The authors acknowledge Nitte (Deemed to be University), Mangaluru, Karnataka, India, for providing the facilities to carry out this work. The authors are also thankful to Lipoid®, GmbH, Germany, for providing the EPC (Lipoid® E 80 S) as a gift sample for this research work. Facilities provided towards the research work by Mangalore University, National Institute of Technology, Karnataka (NITK) and Manipal Academy of Higher Education are also gratefully acknowledged.

COMPLIANCE WITH ETHICAL STANDARDS

Conflict of Interest The authors declare that they have no conflict of interest.

REFERENCES

1. Kandaswami C, Middleton E. Free radical scavenging and antioxidant activity of plant flavonoids. Adv Exp Med Biol. 1994;366:351–76. Available from:. https://doi.org/10.1007/978-1-4615-1833-4_25.
2. Di Perri T, Auteri A. Action of s 5682 on the complement system. In vitro and in vivo study. Int Angiol. 1988;7(2 Suppl):11–5 Available from: http://www.ncbi.nlm.nih.gov/pubmed/3183451.
3. Dung TD, Day CH, Binh TV, Lin CH, Hsu HH, Su CC, et al. PP2A mediates diosmin p53 activation to block HA22T cell proliferation and tumor growth in xenografted nude mice through PI3K-Akt-MDM2 signaling suppression. Food Chem Toxicol. 2012;50(5):1802–10. https://doi.org/10.1016/j.fct.2012.01.
4. Izzo AA, di Carlo G, Mascolo N, Capasso F, Autore G. Antiulcer effect of flavonoids. Role of endogenous PAF. Phyther Res. 1994;8:179–81. https://doi.org/10.1002/ptr.2650080313.
5. Manner S, Skogman M, Goeres D, Vuorela P, Fallarero A. Systematic exploration of natural and synthetic flavonoids for the inhibition of Staphylococcus aureus biofilms. Int J Mol Sci. 2013;14(10):19434–51. https://doi.org/10.3390/ijms141019434.
6. Cushnie TPT, Lamb AJ. Antimicrobial activity of flavonoids. Int J Antimicrob Agents. 2005;26(5):343–56. https://doi.org/10.1016/j.ijantimicag.2005.09.002.
7. Friedman M. Overview of antibacterial, antitoxin, antiviral, and antifungal activities of tea flavonoids and teas. Mol Nutr Food Res. 2007;51(1):116–34. https://doi.org/10.1002/mnfr.200600173.
8. Mukerjee A, Vishwanatha JK. Formulation, characterization and evaluation of curcumin-loaded PLGA nanospheres for cancer therapy. Anticancer Res. 2009;29(10):3867–75.
9. Ravi G, Chandur V, Shabaraya A, Sanjay K. Phytosomes: an advanced herbal drug delivery system. Int J Pharm Res Bio-Sci. 2015;4(3):415–32 Available from: http://www.ijprbs.com/issuedocs/2015/6/IJPRBS%201078.pdf.
10. Mukherjee PK, Wahile A. Integrated approaches towards drug development from Ayurveda and other Indian system of medicines. J Ethnopharmacol. 2006;103(1):25–35. https://doi.org/10.1016/j.jep.2005.09.024.
11. Li F, Yang X, Yang Y, Li P, Yang Z, Zhang C. Phospholipid complex as an approach for bioavailability enhancement of

echinacoside. Drug Dev Ind Pharm. 2015;41(11):1777–84. https://doi.org/10.3109/03639045.2015.1004183.
12. Kalepu S, Manthina M, Padavala V. Oral lipid-based drug delivery systems—an overview. Acta Pharm Sin B. 2013;3(6):361–72. https://doi.org/10.1016/j.apsb.2013.10.001.
13. Yeap YY, Trevaskis NL, Porter CJH. Lipid absorption triggers drug supersaturation at the intestinal unstirred water layer and promotes drug absorption from mixed micelles. Pharm Res. 2013;30(12):3045–58. https://doi.org/10.1007/s11095-013-1104-6.
14. Jiang Q, Yang X, Du P, Zhang H, Zhang T. Dual strategies to improve oral bioavailability of oleanolic acid: enhancing water-solubility, permeability and inhibiting cytochrome P450 isozymes. Eur J Pharm Biopharm. 2016;99:65–72. https://doi.org/10.1016/j.ejpb.2015.11.013.
15. Pouton CW. Formulation of poorly water-soluble drugs for oral administration: physicochemical and physiological issues and the lipid formulation classification system. Eur J Pharm Sci. 2006;29(3–4):278–87. https://doi.org/10.1016/j.ejps.2006.04.016.
16. Li J, Wang X, Zhang T, Wang C, Huang Z, Luo X, et al. A review on phospholipids and their main applications in drug delivery systems. Asian J Pharm Sci. 2015;10(2):81–98. https://doi.org/10.1016/j.ajps.2014.09.004.
17. Khan MS, Krishnaraj K. Phospholipids: a novel adjuvant in herbal drug delivery systems. Crit Rev Ther Drug Carrier Syst. 2014;31(5):407–28. https://doi.org/10.1615/CritRevTherDrugCarrierSyst.2014010634.
18. Maiti K, Mukherjee K, Gantait A, Saha BP, Mukherjee PK. Enhanced therapeutic potential of naringenin-phospholipid complex in rats. J Pharm Pharmacol. 2006;58(9):1227–33. https://doi.org/10.1211/jpp.58.9.0009.
19. Maiti K, Mukherjee K, Gantait A, Saha BP, Mukherjee PK. Curcumin-phospholipid complex: preparation, therapeutic evaluation and pharmacokinetic study in rats. Int J Pharm. 2007;330(1–2):155–63. https://doi.org/10.1016/j.ijpharm.2006.09.025.
20. Yanyu X, Yunmei S, Zhipeng C, Qineng P. The preparation of silybin-phospholipid complex and the study on its pharmacokinetics in rats. Int J Pharm. 2006;307(1):77–82. 17. https://doi.org/10.1016/j.ijpharm.2005.10.001.
21. Tedesco D, Steidler S, Galletti S, Tameni M, Sonzogni O, Ravarotto L. Efficacy of silymarin-phospholipid complex in reducing the toxicity of aflatoxin B1in broiler chicks. Poult Sci. 2004;83(11):1839–43. https://doi.org/10.1093/ps/83.11.1839.
22. Maiti K, Mukherjee K, Gantait A, Nazeer Ahamed H, Saha BP, KumarMukherjee P. Enhanced therapeutic benefit of quercetinphospholipid complex in carbon tetrachloride-induced acute liver injury in rats: a comparative study. Iran J Pharmacol Ther. 2005;4(2):84–90 Available from: http://www.bioline.org.br/pdf?pt05019.
23. Dhase AS, Saboo SS. Preparation and evaluation of phytosomes containing methanolic extract of leaves of Aegle marmelos (Bael). Int J PharmTech Res. 2015;8(6):231–40 Available from: http://sphinxsai.com/2015/ph_vol8_no6/2/(231-240)V8N6PT.pdf.
24. Elgindy N, Elkhodairy K, Molokhia A, Elzoghby A. Lyophilization monophase solution technique for improvement of the physicochemical properties of an anticancer drug, flutamide. Eur J Pharm Biopharm. 2010;74(2):397–405. https://doi.org/10.1016/j.ejpb.2009.11.011.
25. Freag MS, Elnaggar YSR, Abdallah OY. Lyophilized phytosomal nanocarriers as platforms for enhanced diosmin delivery: optimization and ex vivo permeation. Int J Nanomedicine. 2013;8:2385–97. https://doi.org/10.2147/IJN.S45231.
26. Sri KV, Kondaiah A, Ratna JV, Annapurna A. Preparation and characterization of quercetin and rutin cyclodextrin inclusion complexes. Drug Dev Ind Pharm. 2007;33(3):245–53. https://doi.org/10.1080/03639040601150195.
27. Ravi, Chandur V, Shabaraya R, Sanjay. Design and characterization of phytosomal nano carriers for enhanced rutin delivery. Am J PharmTech Res. 2015;5(4):483–95 Available from: https://ajptr.com/archive/volume-5/august-2015-issue-4/54040.html.
28. Singh D, Rawat MS, Semalty A, Semalty M. Quercetin-phospholipid complex: an amorphous pharmaceutical system in herbal drug delivery. Curr Drug Discov Technol. 2012;9(1):17–24. https://doi.org/10.2174/157016312799304507.
29. Bhattacharyya S, Ahammed SM, Saha BP, Mukherjee PK. The gallic acid-phospholipid complex improved the antioxidant potential of gallic acid by enhancing its bioavailability. AAPS PharmSciTech. 2013;14(3):1025–33. https://doi.org/10.1208/s12249-013-9991-8.
30. Sanghavi N, Bhosale SD, Malode Y, Sanghavi N. RP-HPLC method development and validation of quercetin isolated from the plant Tridax procumbens L. J Sci Innov Res. 2014;3(6):594–7 Available from: http://www.jsirjournal.com/Vol3_Issue6_09.pdf.
31. Jain S, Valvi PU, Swarnakar NK, Thanki K. Gelatin coated hybrid lipid nanoparticles for oral delivery of amphotericin B. Mol Pharm. 2012;9(9):2542–53. https://doi.org/10.1021/mp300320d.
32. Jamuna S, Paulsamy S, Karthika K. Screening of in vitro antioxidant activity of methanolic leaf and root extracts of hypochaeris radicata L. (Asteraceae). J Appl Pharm Sci. 2012;2(7):149–54 Available from: http://www.japsonline.com/admin/php/uploads/563_pdf.pdf.
33. Maiti K, Mukherjee K, Murugan V, Saha BP, Mukherjee PK. Exploring the effect of hesperetin-HSPC complex—a novel drug delivery system on the in vitro release, therapeutic efficacy and pharmacokinetics. AAPS PharmSciTech. 2009;10(3):943–50. https://doi.org/10.1208/s12249-009-9282-6.
34. Zhang K, Zhang M, Liu Z, Zhang Y, Gu L, Hu G, et al. Development of quercetin-phospholipid complex to improve the bioavailability and protection effects against carbon tetrachloride-induced hepatotoxicity in SD rats. Fitoterapia. 2016;113:102–9. https://doi.org/10.1016/j.fitote.2016.07.008.
35. Nema A, Agarwal A, Kashaw V. Hepatoprotective activity of leptadenia reticulata stems against carbon tetrachloride-induced hepatotoxicity in rats. Indian J Pharmacol. 2011;43(3):254–7. https://doi.org/10.4103/0253-7613.81507.
36. Sweetman SC. Martindale: the complete drug reference. 36th ed. London: Pharmaceutical Press; 2009.
37. Grit M, Crommelin DJ. Chemical stability of liposomes: implications for their physical stability. Chem Phys Lipids. 1993;64(1–3):3–18. https://doi.org/10.1016/0009-3084(93)90053-6.
38. Hou Z, Li Y, Huang Y, Zhou C, Lin J, Wang Y, et al. Phytosomes loaded with mitomycin C-soybean phosphatidylcholine complex developed for drug delivery. Mol Pharm. 2013;10(1):90–101. https://doi.org/10.1021/mp300489p.
39. Teagarden DL, Baker DS. Practical aspects of lyophilization using non-aqueous co-solvent systems. Eur J Pharm Sci. 2002;15(2):115–33. https://doi.org/10.1016/S0928-0987(01)00221-4.
40. Telang DR, Patil AT, Pethe AM, Tatode AA, Anand S, Dave VS. Kaempferol-phospholipid complex: formulation, and evaluation of improved solubility, in vivo bioavailability, and antioxidant potential of kaempferol. J Excipients and Food Chem. 2016;7(4):89–116 Available from: http://fisherpub.sjfc.edu/pharmacy_facpub.
41. Salazar J, Heinzerling O, Müller RH, Möschwitzer JP. Process optimization of a novel production method for nanosuspensions using design of experiments (DoE). Int J Pharm. 2011;420(2):395–403. https://doi.org/10.1016/j.ijpharm.2011.09.003.38.
42. Xu K, Liu B, Ma Y, Du J, Li G, Gao H, et al. Physicochemical properties and antioxidant activities of luteolin-phospholipid complex. Molecules. 2009;14(9):3486–93. https://doi.org/10.3390/molecules14093486.
43. Kemp W. Organic spectroscopy. In: Infrared spectroscopy. 3rd ed. New York: Palgrave; 1991. p. 19–99. Available from: https://link.springer.com/content/pdf/bfm%3A978-1-349-15203-2%2F1.pdf.
44. Georgeta S, Pana PI, Tunde H, Sanda B. The isolation and identification of rutin from pharmaceutical products. Analele Univ Din Oradea Fasc Ecotoxicologie, Zooteh Si Tehnol Ind Aliment. 2016:109–13 Available from: https://www.cabdirect.org/cabdirect/abstract/20173102478.
45. Semalty A, Semalty M, Singh D, Rawat MSM. Preparation and characterization of phospholipid complexes of naringenin for effective drug delivery. J Incl Phenom Macrocycl Chem. 2010;67(3–4):253–60. https://doi.org/10.1007/s10847-009-9705-8.
46. Chen Y, Chen J, Cheng Y, Luo L, Zheng P, Tong Y, et al. A lyophilized sterically stabilized liposome-containing docetaxel: in vitro and in vivo evaluation. J Liposome Res. 2017;27(1):64–73. https://doi.org/10.3109/08982104.2016.1158185.
47. Telange DR, Patil AT, Pethe AM, Fegade H, Anand S, Dave VS. Formulation and characterization of an apigenin-

phospholipid phytosome (APLC) for improved solubility, in vivo bioavailability, and antioxidant potential. Eur J Pharm Sci. 2017;108:36–49. https://doi.org/10.1016/j.ejps.2016.12.009.
48. Adebiyi OE, Olayemi FO, Ning-Hua T, Guang-Zhi Z. In vitro antioxidant activity, total phenolic and flavonoid contents of ethanol extract of stem and leaf of Grewia carpinifolia. Beni-Suef Univ J Basic Appl Sci. 2017;6(1):10–4. https://doi.org/10.1016/j.bjbas.2016.12.003.
49. Wu Y, Wang F, Zheng Q, Lu L, Yao H, Zhou C, et al. Hepatoprotective effect of total flavonoids from Laggera alata against carbon tetrachloride-induced injury in primary cultured neonatal rat hepatocytes and in rats with hepatic damage. J Biomed Sci. 2006;13(4):569–78. https://doi.org/10.1007/s11373-006-9081-y.
50. Khan RA, Khan MR, Sahreen S. CCl4-induced hepatotoxicity: protective effect of rutin on p53, CYP2E1 and the antioxidative status in rat. BMC Complement Altern Med. 2012;12:178. https://doi.org/10.1186/1472-6882-12-178.
51. Abou Seif HS. Physiological changes due to hepatotoxicity and the protective role of some medicinal plants. Beni-Suef Univ J Basic Appl Sci. 2016;5(2):134–46. https://doi.org/10.1016/j.bjbas.2016.03.004.
52. Horváthová K, Novotný L, Tóthová D, Vachálková A. Determination of free radical scavenging activity of quercetin, rutin, luteolin and apigenin in H2O2-treated human ML cells K562. Neoplasma. 2004;51(5):395–9.
53. Kim HJ, Bruckner JV, Dallas CE, Gallo JM. Effect of dosing vehicles on the pharmacokinetics of orally administered carbon tetrachloride in rats. Toxicol Appl Pharmacol. 1990;102(1):50–60. https://doi.org/10.1016/0041-008X(90)90082-6.
54. Glende EA, Hruszkewycz AM, Recknagel RO. Critical role of lipid peroxidation in carbon tetrachloride-induced loss of aminopyrine demethylase, cytochrome P-450 and glucose 6-phosphatase. Biochem Pharmacol. 1976;25(19):2163–70. https://doi.org/10.1016/0006-2952(76)90128-3.
55. Recknagel RO, Glende EA, Dolak JA, Waller RL. Mechanisms of carbon tetrachloride toxicity. Pharmacol Ther. 1989;43(1):139–54. https://doi.org/10.1016/0163-7258(89)90050-8.
56. Amić A, Lučić B, Stepanić V, Marković Z, Marković S, Dimitrić Marković JM, et al. Free radical scavenging potency of quercetin catecholic colonic metabolites: thermodynamics of 2H + /2e− processes. Food Chem. 2017;218:144–51. https://doi.org/10.1016/j.foodchem.2016.09.018.
57. Althnaian T, Albokhadaim I, El-Bahr SM. Biochemical and histopathological study in rats intoxicated with carbontetrachloride and treated with camel milk. Springerplus. 2013;2(1):57. https://doi.org/10.1186/2193-1801-2-57.
58. Li J, Liu P, Liu JP, Yang JK, Zhang WL, Fan YQ, et al. Bioavailability and foam cells permeability enhancement of Salvianolic acid B pellets based on drug-phospholipids complex technique. Eur J Pharm Biopharm. 2013;83(1):76–86. https://doi.org/10.1016/j.ejpb.2012.09.021.
59. Freag MS, Saleh WM, Abdallah OY. Self-assembled phospholipid-based phytosomal nanocarriers as promising platforms for improving oral bioavailability of the anticancer celastrol. Int J Pharm. 2018;535(1–2):18–26. https://doi.org/10.1016/j.ijpharm.2017.10.053.